REPORT 455

ADVISORY GROUP FOR AERONAUTICAL RESEARCH AND DEVELOPMENT

64 RUE DE VARENNE, PARIS VII

REPORT 455

PROPERTIES OF THE FLUCTUATING WALL-PRESSURE FIELD OF A TURBULENT BOUNDARY LAYER

by

M. K. BULL

APRIL 1963

NORTH ATLANTIC TREATY ORGANIZATION

REPORT 455

NORTH ATLANTIC TREATY ORGANIZATION

ADVISORY GROUP FOR AERONAUTICAL RESEARCH AND DEVELOPMENT

PROPERTIES OF THE FLUCTUATING WALL-PRESSURE FIELD OF A TURBULENT BOUNDARY LAYER

by

M.K. Bull

This Report is one in the Series 448-469 inclusive, presenting papers, with discussions, given at the AGARD Specialists' Meeting on 'The Mechanism of Noise Generation in Turbulent Flow' at the Training Center for Experimental Aerodynamics, Rhode-Saint-Genèse, Belgium, 1-5 April 1963, sponsored by the AGARD Fluid Dynamics Panel

SUMMARY

- The results of measurements of various statistical properties of the fluctuating wall-pressure field associated with turbulent subsonic boundary layer flow in conditions covering a range of values of boundary layer thickness and flow speed are given. The measured quantities include overall rms pressures, frequency spectra, and longitudinal and lateral space-time correlations in both broad and narrow frequency bands. Some experimental values of space-time correlation between wall-pressure fluctuations and turbulent velocity fluctuations at various positions in the boundary layer are also presented.

These experimental results and some of their implications on the structure of the wall-pressure field and the nature of its convection and decay are discussed.

SOMMAIRE

On donne les résultats de mesures de diverses propriétés statistiques du champ de pression de paroi variable associé à l'écoulement des couches limitrophes turbulentes subsoniques dans des conditions englobant une plage de valeurs d'épaisseurs de couches limitrophes et de vitesse d'écoulement. Les quantités mesurées sont entre autres les pressions totales racine de moyenne des carrés, les spectres de fréquence et les corrélations espace-temps longitudinales et latérales tant dans les bandes de fréquences larges qu'étroites. On présente aussi quelques valeurs expérimentales de corrélation espace-temps entre les fluctuations de pression à la paroi et les fluctuations de vitesse de turbulence à diverses positions dans la couche limitrophe.

On discute ces résultats expérimentaux et certaines de leurs implications sur la structure du champ de pression à la paroi et la nature de sa convection et sa décroissance.

532.526.4
3b2f:3b2e1a

CONTENTS

LIST OF FIGURES

NOTATION

C_f	skin friction coefficient = τ_0/q_0
d	diameter of pressure transducer
H	boundary layer form parameter = δ^*/θ
M_0	free stream Mach number
p	fluctuating component of static pressure on the wall
p'	root mean square wall pressure = $\langle p^2 \rangle$
q_0	free stream dynamic pressure = $\frac{1}{2}\rho_0 U_0^2$
$Q_{pp}(\xi_1,\xi_3,\tau)$	wall pressure covariance (Equation (2))
$Q_{pp}^{\omega}(\xi_1,\xi_3,\tau)$	covariance of narrow band wall pressure signals
$R_{e\theta}$	Reynolds number = $U_0\theta/\nu$
$R_{pp}(\xi_1,\xi_3,\tau)$	wall-pressure correlation coefficient (Equation (4))
$R_{pp}^{\omega}(\xi_1,\xi_3,\tau)$	correlation coefficient of narrow band wall-pressure signals
$R_{pu_1}(\xi_1,\xi_2,\xi_3,\tau)$	pressure-velocity correlation coefficient (Equation (14))
u_i	fluctuating velocity component in x_i direction
u_1'	root mean square velocity fluctuation in stream direction = $\langle u_1^2 \rangle$
U	mean velocity in flow direction
U_c	average convection velocity
U_c'	instantaneous convection velocity
$U_c(\omega)$	convection velocity derived from narrow band correlation measurements
U_0	mean flow velocity outside boundary layer
U_τ	friction velocity = $\sqrt{(\tau_0/\rho_0)}$
x_1	co-ordinate in the direction of mean flow
x_2	co-ordinate normal to wall

x_3	co-ordinate transverse to flow
y	distance normal to wall
δ^*	displacement thickness of boundary layer
$\phi_p(\omega)$	power spectral density of wall-pressure fluctuations
$\phi_{pp}(\xi_1,\xi_3,\omega)$	spectral function (Equation (5))
τ	time delay
τ_c	convection time
τ_0	wall shear stress
θ	momentun thickness of boundary layer
ω	circular frequency
ρ_0	free stream density
ν	kinematic viscosity
ξ_1,ξ_2,ξ_3	separation distances in x_1, x_2, x_3 directions

PROPERTIES OF THE FLUCTUATING WALL-PRESSURE FIELD OF A TURBULENT BOUNDARY LAYER

M.K. Bull*

1. INTRODUCTION

Wall pressure fluctuations produced by a turbulent boundary layer have been the subject of many investigations. Early experimental work was, on the whole, confined to measurement of the root mean square and frequency spectrum of the wall pressure, and in many cases the instrumentation available did not give an adequate coverage of the band-width of the fluctuations. More recently the development of miniature pressure transducers and the extensive use of correlation techniques has led to a much more detailed examination of the wall pressure field, and its relation to turbulent velocity fluctuations in the boundary layer.

The experimental results presented in this Report show that space-time correlations of the overall pressure signals, supplemented by correlations in narrow frequency bands, can provide a considerable amount of information on details of the structure of the pressure field. Additional information on the relation between the wall pressure field and velocity fluctuations in the boundary layer is provided by correlating the outputs of a pressure transducer in the wall and a hot-wire anemometer in the boundary layer.

2. THE WIND TUNNEL

The experimental data which are presented in this Report were obtained from measurements made on the turbulent boundary layer developed on one of the ground and polished 9-inch walls of the subsonic test section of the 9 inch x 6 inch boundary layer tunnel in the University of Southampton.

This wind tunnel is of the induced flow non-return type driven by the injection of compressed air downstream of the working sections. It has two working sections, a subsonic section 10 feet long followed by a supersonic section 6 feet long, both of which have rectangular cross-sections nominally 9 inches x 6 inches. The working sections are of fairly massive steel construction, are mechanically independent, and carried on anti-vibration mountings. The subsonic section is slightly divergent to compensate for boundary layer growth and so that there is no pressure gradient along it. Instrumentation has to be mounted in 6-inch diameter plugs which fit ports in one of the 9-inch walls. The general arrangement of the tunnel is shown in Figure 20.

To keep the extraneous sound field in the test section to a minimum, injector and diffuser are heavily sound-proofed and in the present experiments the tunnel was always run in a choked condition so that injector and diffuser noise were not propagated internally into the test section. The diffuser outlet is outside the laboratory building.

---

*Department of Aeronautics, The University of Southampton, Southampton, England

3. INSTRUMENTATION

All measurements of fluctuating pressures were made with piezoelectric transducers set flush in the wind tunnel wall. The pressure-sensitive elements were lead zirconate-titanate disks, 0.030 inch in diameter.

The pressure transducers were mounted rigidly in their instrument plugs, the mass of the side-plates of the wind tunnel being relied upon to keep vibration of the instruments down to an acceptable value.

The electrical output of the transducer was fed to a pre-amplifier with high input impedance and the signal then further amplified for direct spectral analysis (Bruel and Kjäer ⅓-octave Audio Frequency Spectrometer, Type 2111) or for recording on magnetic tape (Ampex Model FR-100). All correlation values were obtained from recorded signals processed by the correlation equipment described in Reference 1.

Calibration of a transducer was effected by first mounting it in the wall of a shock tube and checking the overall linearity by means of the response to the passage of a shock wave across its face. A detailed low frequency response was then obtained by calibration against a standard condenser microphone, the two instruments being mounted in a small cavity together with a moving coil hearing aid which was used as the calibration signal generator. With the latter procedure the transducer could be calibrated in its experimental mounting. The calibration was normally checked before and after each tunnel run when root mean square pressure and spectral density measurements were being made.

Velocity fluctuations were measured by a constant temperature hot-wire anemometer (Disa Type 55 A 01). The hot-wires were tungsten, 0.0002 inch in diameter. The wires were welded to their supports and subsequently copper plated leaving an unplated working length of 0.06 inch. The hot wire probes were carried on supports of aerofoil section which could be traversed normal to the tunnel wall.

4. THE FLOW UNDER INVESTIGATION AND ASSOCIATED EXPERIMENTAL CONDITIONS

4.1 Boundary Layer Characteristics

Measurements of wall pressure fluctuations were made for two free stream Mach numbers, $M_0 = 0.3$ and 0.5 . The variation of displacement thickness, δ^* , and momentum thickness, θ , of the boundary layer along the working section for these two flow conditions is shown in Figures 1 and 2. These Figures also show the variation of the form parameter $H = \delta^*/\theta$. The corresponding values of Reynolds number and skin friction are given by Figures 3 and 4.

Skin friction values were derived from the slopes of the measured velocity profiles using the law of the wall,

$$\frac{U}{U_\tau} = \frac{1}{K}\ln\left(\frac{yU_\tau}{\nu}\right) + B \qquad (1)$$

with $K = 0.40$.

Velocity profiles were obtained from Pitot tube and wall static pressure measurements. For both flow Mach numbers a satisfactory collapse of velocity profile data from various stations along the test section was obtained in velocity defect form in terms of the derived skin friction values. The plot of $(U_0 - U)/U_\tau$ versus y/δ for $M_0 = 0.5$ is shown in Figure 5.

The intensity of the longitudinal component of residual turbulence in the free stream outside the boundary layer was measured only for $M_0 = 0.5$. The value found was $u'/U_0 = 2.0 \times 10^{-3}$ with virtually no variation along the length of the working section.

4.2 Sources of Extraneous Pressure Signals

The two effects most likely to give rise to interference with the wall pressure measurements are vibration of the working section of the wind tunnel and the presence of a sound field in the working section.

Measurements of the spectrum of the output of the transducer when it was mounted in the tunnel wall but blanked off from the flow showed that vibration effects were sufficiently small to be neglected.

On the other hand the sound field in the working section was not negligible under all measuring conditions. The intensity of this field in the free stream was measured by means of a faired ½-inch condenser microphone. It was established that the introduction of the microphone itself produced no significant increase in the internal sound intensity by means of a monitor microphone located flush with the wall of the settling chamber, upstream of the contraction leading to the working section (it had been found, previously, that acoustic disturbances in the working section produced by the introduction of measuring apparatus such as Pitot tubes and hot-wire probes could be quite readily detected by a microphone in this position). The sound intensity registered by the faired microphone therefore represented the internal sound field of the empty tunnel plus possibly some small increase due to the disturbance effect of the microphone itself.

The sound pressure level in the test section was found to increase with increasing distance downstream for both $M_0 = 0.3$ and 0.5, the increase being about 5 decibels from upstream to downstream end of the working section. For most test conditions the mean square acoustic pressure was less than 4 per cent of the mean square wall pressure, although in the worst case, which occurred at the downstream end of the working section at $M_0 = 0.5$, this figure approached 9 per cent.

The microphone signal had a broad band character, the spectral density being highest at low frequencies and falling off with increasing frequency. Because of the high spectral density of this background field at low frequencies, the spectral density measurements of the pressure field were rejected for frequencies less than 300 cycles/sec. This low frequency cut-off amounts to a Strouhal number limitation of 0.01 to 0.06 depending on the flow conditions. The recorded signals for correlation purposes were also cut off at this frequency by making use of the response characteristics of the tape recorder. The bandwidth of recorded signals was 300 to 30,000 cycles/sec.

5. ROOT MEAN SQUARE AND FREQUENCY POWER SPECTRUM OF THE WALL PRESSURE FLUCTUATIONS

The statistical properties of the wall-pressure field to be discussed are all particular values of the covariance

$$Q_{pp}(\xi_1,\xi_3,\tau) = \langle p(x_1,x_3,t)\ p(x_1+\xi_1,\ x_3+\xi_3,\ t+\tau)\rangle \tag{2}$$

(where $\langle\ \rangle$ denotes a statistical mean value) or of spectral functions derived from it.

Equation (2) can be normalised by dividing it by the mean square pressure

$$(p')^2 = \langle p^2\rangle = Q_{pp}(0,0,0) \tag{3}$$

to give the correlation coefficient

$$R_{pp}(\xi_1,\xi_3,\tau) = \frac{Q_{pp}(\xi_1,\xi_3,\tau)}{\langle p^2\rangle}\ . \tag{4}$$

The Fourier transform of Q_{pp} with respect to time yields the spectral function

$$\phi_{pp}(\xi_1,\xi_3,\omega) = \frac{1}{2\pi}\int_{-\infty}^{\infty} Q_{pp}(\xi_1,\xi_3,\tau)e^{-i\omega\tau}\,d\tau \tag{5}$$

the inverse relation being

$$Q_{pp}(\xi_1,\xi_3,\tau) = \int_{-\infty}^{\infty}\phi_{pp}(\xi_1,\xi_3,\omega)\ e^{i\omega\tau}\,d\omega\ . \tag{6}$$

The frequency power spectral density $\phi_p(\omega)$ of the pressure fluctuations, as measured by a wave-analyser, is given by

$$\phi_p(\omega) = \phi_{pp}(0,0,\omega) + \phi_{pp}(0,0,-\omega)$$

$$= \frac{2}{\pi}\int_0^{\infty} Q_{pp}(0,0,\tau)\cos\omega\tau\,d\tau\ . \tag{7}$$

It was hoped that measurements of root mean square pressure at various stations along the working section at the two free stream Mach numbers $M_0 = 0.3$ and 0.5 would give an indication of the effect of Reynolds number on this parameter. However, even with the small transducer elements used, for which the ratio of transducer diameter to boundary layer thickness was in the range $0.17 < d/\delta^* < 0.52$, the real effects of Reynolds number seem to have been obscured by the effects of transducer resolution.

The measured values of p'/q_0 and p'/τ_0 are shown in Figure 6. At both flow Mach numbers the value of p'/q_0 was found to increase as the measuring station was moved downstream along the test section. Since the corresponding value of skin friction coefficient C_f decreases (Figs. 3 and 4), there is an even more rapid increase in the ratio of rms pressure to wall shear stress p'/τ_0. In fact the value of p'/τ_0 increases by about 40 per cent for a Reynolds number change by a factor of about 4. In contrast to this behaviour the values of p'/τ_0 found by various previous investigators suggest a decrease with increasing Reynolds number (see for example the summary given in Reference 2) although the trend is by no means well established, largely because of the diversity of experimental conditions. For pipe flow Corcos[3] finds a slow decrease of p'/τ_0 with increasing Reynolds number.

The data for the frequency power spectrum of the pressure, expressed in non-dimensional form, $\phi_p(\omega)U_0/q_0^2\delta^*$, in terms of the dynamic pressure and velocity of the stream outside the boundary layer and displacement thickness, are shown in Figure 7. They collapse quite well at low and intermediate frequencies, $\omega\delta^*/U_0 < 1$, but at higher frequencies there is a spread of values, consistent with an increasing attenuation (due to finite transducer size) with increasing d/δ^*. It is fairly clear, therefore, that a large part of the observed increase in p'/τ_0 with Reynolds number is due to the parallel decrease in size of the transducer relative to the scale of the pressure field.

However, if we assume that where the measured spectra fall on a single non-dimensional curve ($\omega\delta^*/U_0 < 1$) the effects of finite size of transducer are negligible, there remains an indication that over this region spectral density expressed in terms of wall shear stress in the form $\phi_p(\omega)U_0/q_0^2\delta^*$ increases with Reynolds number although at a considerably smaller rate than suggested by the rms pressure measurements.

At $M_0 = 0.5$ the value of p'/τ_0 at the smallest experimental value of d/δ^* (namely 0.17) was 2.68 whilst at $M_0 = 0.3$ the smallest value of d/δ^* was 0.16 and the corresponding p'/τ_0 was 2.53.

6. OVERALL SPACE-TIME CORRELATIONS

Overall space-time correlations $R_{pp}(\xi_1, \xi_3, \tau)$ were measured for various transducer separations along lines making angles of 0^0, 30^0, 60^0 and 90^0 with the mean flow direction at $M_0 = 0.3$ and 0^0 and 90^0 at $M_0 = 0.5$. The flow conditions for these measurements are summarised in Table I. A typical set of curves of the longitudinal space-time correlation, $R_{pp}(\xi_1, 0, \tau)$, as a function of non-dimensional time delay $U_0\tau/\delta^*$, for various values of ξ_1/δ^*, are shown in Figure 8.

6.1 Space Correlations

The values of the longitudinal space correlation, $R_{pp}(\xi_1, 0, 0)$, for a variety of flow conditions are shown in Figure 9 as a function of the non-dimensional spatial separation ξ_1/δ^*. The points can be reasonably well represented by a single curve. The longitudinal correlation is negative for spatial separations greater than about $3.9\delta^*$, while the lateral correlation, $R_{pp}(0, \xi_3, 0)$, shown in Figure 10, remains positive at the largest value of ξ_3/δ^* investigated. Correlations along lines at

angles of 30^{o} and 60^{o} to the free stream flow direction for $M_0 = 0.3$ (Fig. 11) have intermediate forms.

TABLE I

M_0	δ^* (inches)	$R_{e\theta}$	H
0.3	0.081	10,100	1.36
0.3	0.149	19,400	1.31
0.5	0.057	10,900	1.39
0.5	0.126	24,300	1.37
0.5	0.173	33,800	1.36

From the space correlation curves for the four angles to the flow (Fig. 11), the correlation pattern of the pressure field can be mapped out as a set of isocorrelation contours. Figure 12 shows the resulting pattern. If the long tail of the lateral correlation curve is accepted, the scale of the pressure field in the lateral direction is considerably greater than the longitudinal scale, and this is clearly shown by the isocorrelation contours of the field. The integral lateral scale, $\int_0^\infty R_{pp}(0,\xi_3,0)d\xi_3$, is about three times as great as the longitudinal scale $\int_0^\infty R_{pp}(\xi_1,0,0)d\xi_1$. At large separations the accuracy of determination of the correlation coefficients is not high and the results are more likely to be influenced by extraneous effects such as the background sound field in the wind tunnel, so the disparity in scales may not be quite as large as indicated above. However, the results certainly indicate anisotropy of the pressure field with the lateral scale exceeding the longitudinal.

6.2 Space-Time Correlations and Convection Velocity

If we take the position of the centre of a pressure eddy after a lapse of time τ to be that value of ξ_1 for which the correlation with the original signal $R_{pp}(\xi_1,0,\tau)$

is a maximum at the instant τ then $U_c = \xi_1/\tau$ represents an average velocity of the eddy over the period τ. This same velocity U_c can equally well be derived from the envelope of the curves of $R_{pp}(\xi_1, 0, \tau)$ versus τ for various values of ξ_1 = constant. A typical set of these curves is shown in Figure 13. The convection velocity is now given by

$$U_c = \frac{\xi_1}{\tau_c} \tag{8}$$

where τ_c is the time delay for which the curve ξ_1 = constant touches the envelope.

The instantaneous convection velocity, U_c', of the pressure field is given by the slope of the ξ_1 versus τ_c curve

$$U_c' = \frac{d\xi_1}{d\tau_c} . \tag{9}$$

This distinction between average and instantaneous velocities has to be made since it is found that the relation between ξ_1 and τ_c is not linear, as Figure 14 shows. In fact, as will be seen from Figure 15, the convection velocity increases markedly with increasing spatial separation from a value less than $0.6\,U_0$ at very small separations to a value in excess of $0.8\,U_0$ at large separations. The asymptotic values of U_c/U_0 found in the present experiments are 0.53 and 0.825 for small and large separations respectively.

If the convection velocity is determined in the same way from correlations for which $\xi_3 \neq 0$ it is found that the initial rise with increasing spatial separation is even more rapid than for the $\xi_3 = 0$ case (Fig. 15).

A feature of the space-time correlation curves with increasing ξ_1 is that, in addition to the maximum value of correlation coefficient becoming smaller, the curves quickly lose their sharp peaks and become much broader (for example, Figure 8). This indicates that the spectrum of the correlation-producing wave-number components is becoming progressively curtailed at the high wave-number end, and further that each particular wave-number component loses coherence in the time taken for it to travel a distance which is broadly proportional to its wave-length.

This behaviour considered in conjunction with the observed variation in convection velocity indicates that the high wave-number (small-scale) components of the pressure field are convected downstream slowly at speeds of the order of $0.5\,U_0$ and rapidly lose their coherence while the low wave-number (large-scale) components are convected rapidly at speeds typically of the order of 0.8 to $0.9\,U_0$ and lose coherence quite slowly.

7. NARROW-BAND SPACE-TIME CORRELATIONS AND CONVECTION VELOCITIES

More detailed information about the convection velocities and rate of loss of coherence of the various components of the pressure field can be obtained from measurements of correlations of the pressure signals after they have been passed through

narrow-band filters, a method first applied to wall pressure measurements by Harrison[4].

If the covariance of the pressure signals in a narrow frequency band centred on ω is denoted by $Q^{\omega}_{pp}(\xi_1,\xi_3,\tau)$, defined in the same way as $Q_{pp}(\xi_1,\xi_3,\tau)$ (Equation (2)) for the broad-band signal, then we can define a correlation coefficient

$$R^{\omega}_{pp}(\xi_1,\xi_3,\tau) = \frac{Q^{\omega}_{pp}(\xi_1,\xi_3,\tau)}{Q^{\omega}_{pp}(0,0,0)} \tag{10}$$

which is the narrow-band analogue of Equation (4).

It can oe shown[5] that

$$R^{\omega}_{pp}(\xi_1,\xi_3,\tau) = \frac{|\phi_{pp}(\xi_1,\xi_3,\omega)|}{|\phi_{pp}(0,0,\omega)|}\cos(\omega\tau+\alpha)\ , \tag{11}$$

ϕ_{pp} being the (complex) spectral function given by Equation (5). α, the phase angle of $\phi_{pp}(\xi_1,\xi_3,\omega)$, results from the convection of the pressure components in the frequency band being considered. Convection velocities could be determined from the envelope of the major peaks of the curves of R^{ω}_{pp} versus time delay for various constant values of spatial separation, in the same way as for the overall pressure correlations, but it is somewthat more convenient to find convection velocities, $U_c(\omega)$, from the time delays corresponding to the major peaks themselves, i.e. given by

$$\alpha = -\frac{\omega\xi_1}{U_c(\omega)}\ . \tag{12}$$

The values of convection velocity obtained by the two methods will not differ very greatly.

The way in which a particular frequency component loses coherence during the convection process is represented by the behaviour with increasing spatial separation of the amplitude of narrow-band correlation coefficient $|\phi_{pp}(\xi_1,\xi_3,\omega)|/|\phi_{pp}(0,0,\omega)|$ which will be denoted by $|R^{\omega}_{pp}(\xi_1,\xi_3,\tau)|$. Experimental results for the variation of amplitude of the longitudinal narrow-band correlation, $|R^{\omega}_{pp}(\xi_1,0,\tau)|$, are shown in Figure 16; they can be quite accurately represented as a unique function of $\omega\xi_1/U_c(\omega)$ except at low values of this parameter. This type of dependence is untenable at low values of $\omega\xi_1/U_c(\omega)$ since $|R^{\omega}_{pp}(\xi_1,0,\tau)|$ must equal unity at $\xi_1 = 0$ for all ω, but will not equal unity for $\omega = 0$ at non-zero values of ξ_1. The deviation from $\omega\xi_1/U_c(\omega)$ dependence at low values of $\omega\xi_1/U_c(\omega)$ might be expected to occur at higher values of $\omega\xi_1/U_c(\omega)$ the higher the value of ξ_1/δ^*, and this expectation is confirmed by the trends indicated in Figure 16. In Reference 5 an expression for $|R^{\omega}_{pp}(\xi_1,0,\tau)|$ was derived for a pressure field which was a slowly varying function of time in a convected reference frame. $|R^{\omega}_{pp}(\xi_1,0,\tau)|$ was found to be a function of ξ_1/δ^* only, and not frequency dependent. This conclusion, which seems to have been largely a consequence of the particular forms assumed for the correlation functions, becomes increasingly at variance with the present experimental results and those of References 3 and 4 as the values of $\omega\xi_1/U_c(\omega)$ increases, but it may still provide a reasonable representation of the behaviour of the narrow-band correlations at low frequencies where $\omega\xi_1/U_c(\omega)$ dependence is no longer valid.

The fact that the amplitudes of the longitudinal narrow-band correlations behave as a function of $\omega\xi_1/U_c(\omega)$ over a wide range of values of this parameter indicates that, in the main, the loss of coherence of a frequency component occurs in a time which is inversely proportional to its frequency, or, identifying frequency components with convected wave number components by means of the relation

$$\omega = k_1 U_c(\omega), \tag{13}$$

that a wave number component loses coherence in travelling a distance proportional to its wave-length.

The amplitude of the lateral filter band correlations, $\left|R^{\omega}_{pp}(0,\xi_3,\tau)\right|$, in the same way, tends to be a unique function of $\omega\xi_3/U_c(\omega)$ except for small values of $\omega\xi_3/U_c(\omega)$ (Fig. 17), indicating that the lateral coherence of a given longitudinal wave number component is also proportional to its wave-length. As in the longitudinal case the deviations from dependence on $\omega\xi_3/U_c(\omega)$ only are greater the larger the value of ξ_3/δ^*.

Values of the ratio of convection velocity to free-stream velocity are shown in Figure 18 as a function of $\omega\delta^*/U_c(\omega)$. As well as a frequency dependence the values of $U_c(\omega)/U_0$ show a variation with spatial separation of the measuring points, similar to that observed in the case of the overall convection velocity (Fig. 15). A spatial dependence was also found in the low and high frequency measurements reported by Willmarth and Wooldridge in Reference 2.

Figure 18 shows that the increase in $U_c(\omega)/U_0$ with spatial separation occurs mainly for $0 < \xi_1/\delta^* < 5$. At greater values of ξ_1/δ^* there is very little further convection velocity increase.

It has been assumed on several occasions in this Report that fixed point frequencies and longitudinal wave-numbers are interchangeable. It is known that the time scale of the pressure fluctuations in a frame of reference moving with the pressure eddies is very much greater than the time scale in a fixed reference frame, so that the relation given by Equation (13) can be expected to be a good approximation. However, to further identify a given fixed point frequency with one wave-number component (or a very narrow band of wave number components) rather than with a wide range of k_1 all of which are associated with the same value of $k_1 U_c(k_1)$ requires that the convection velocity should be a unique function of k_1. This is equivalent to saying that $U_c(\omega)$ should be a unique function of $\omega\delta^*/U_c(\omega)$. Figure 18 shows that this condition is not precisely satisfied - in fact if this figure is interpreted as $U_c(k_1)/U_c$ versus $k_1\delta^*$ then there will be an uncertainty in $U_c(k_1)/U_0$ associated with a given value of k_1 which is small at small $k_1\delta^*$ but becomes of the order of $\pm$ 10 per cent at large $k_1\delta^*$. But, although there is a range of convection velocities associated with a particular value of k_1, the indications are that it is confined within fairly narrow limits.

The results of the correlation measurements in narrow frequency bands therefore indicate that the pressure field can be regarded as made up by the superposition of longitudinal wave number components with each of which can be associated a reasonably well-defined convection speed or limited range of convection speeds. The various components are coherent over lateral distances which are proportional to their

wave-lengths and retain coherence in the flow direction for times proportional to the times taken for them to be convected distances equal to their wave-lengths.

This conclusion is consistent with the observation of the overall space-time correlation characteristics of the pressure field. It explains the change in character of the correlation with increasing time delay and spatial separation, the variation of convection velocity with increasing spatial separation and the different rates of variation of convection velocity with ξ_1 for different values of ξ_3.

The fact that a more or less unique convection velocity can be assigned to a particular wave number component, suggests that by and large the pressure fluctuations of a particular longitudinal wave number originate from a region of the boundary layer where the mean flow velocity is equal to the observed convection velocity. If longitudinal wave number components k_1 are associated with physical scales this leads to the conclusion that small-scale pressure fluctuations originate from boundary layer turbulence quite close to the wall while the larger-scale fluctuations are associated with motion in the outer regions of the layer. This conclusion might be expected to apply with greater accuracy to the small-scale than to large-scale fluctuations, since the correspondence between the longitudinal wave number k_1 and physical scale tends to lose precision at small values of k_1 ; this is borne out by the fact that the convection velocity of the overall field at large separations does not greatly exceed $0.8U_0$ and that even in narrow frequency bands $U_c(\omega)$ does not exceed $0.9U_0$ for small k_1 , indicating that the sources of fluctuation with low k_1 cannot be so accurately located, but are more widely dispersed throughout the boundary layer, their convection velocities representing an average of a fairly wide range of values.

8. PRESSURE-VELOCITY CORRELATIONS

In an effort to determine how different regions of the boundary layer contribute to the wall pressure field, measurements of the correlation between the wall pressure fluctuations and turbulent velocity fluctuations at various positions in the layer were begun. It was the intention to investigate the correlation between p and u_1 and between p and u_2 , but because of experimental difficulties which are briefly referred to below values of the former correlation only have been obtained.

The coefficient of correlation between p and u_1 is defined as

$$R_{pu_1}(\xi_1,\xi_2,\xi_3,\tau) = \frac{\langle\, p(x_1,x_2,x_3,t)\; p(x_1+\xi_1,x_2+\xi_2,x_3+\xi_3,t+\tau)\,\rangle}{\langle\, p^2(x_1,x_2,x_3)\,\rangle^{\frac{1}{2}}\langle\, u_1^2(x_1+\xi_1,x_2+\xi_2,x_3+\xi_3)\,\rangle^{\frac{1}{2}}} \qquad (14)$$

Values of $R_{pu_1}(\xi_1,\xi_2,0,\tau)$ have been obtained for $0.4 < \xi_2/\delta^* < 4.4$ and $0 < \xi_1/\delta^* < 12.3$ for flow conditions $M_0 = 0.5$ and $\delta^* = 0.126$ inch.

Considerable difficulty was experienced in eliminating the interference effect of the hot-wire probe on the pressure field, even when the wire was located downstream of the pressure transducer. By careful re-design of the hot-wire probe the interference was considerably reduced, to a state where it amounted to only 1 or 2 per cent increase in the output of the pressure transducer. Under these conditions the main effect was an increase in pressure spectral density at low frequencies,

$\omega\delta^*/U_0 < 0.14$, and the pressure and velocity signals were therefore passed through high-pass filters which cut out frequencies below this value.

Typical results for various values of ξ_2/δ^* and $\xi_1/\delta^* = 3.88$ are shown in Figure 19. The correlation curves are asymmetrical, the correlation being zero at the centre of the disturbance which is correlated with the wall pressure. The greatest magnitude reached by the coefficient on either side of its zero-crossing was found to be greatest for small values of ξ_1/δ^* and ξ_2/δ^* and to decrease slowly as these separation distances increased. The slow decrease towards the outer edge of the boundary layer does not necessarily imply that the wall pressure receives comparable contributions from all parts of the boundary layer since the intensity of velocity fluctuation falls off rapidly as the distance from the wall, ξ_2/δ^* , increases. A more realistic indication of the contributions of various parts of the layer to the wall pressure can probably be obtained by considering the variation of $u_1' R_{pu_1}$ across the layer. Since the value of u_1'/U_0 varies from about 0.10 in the inner region of the boundary layer to the residual free-stream value, which in this case was about 2×10^{-3}, the value of $u_1' R_{pu_1}$ falls off quite rapidly with increasing distance from the wall. In relation to its value at about one displacement thickness from the wall, the value at $\xi_2/\delta^* = 5$ is about 10 per cent and at the outer edge of the layer only 1 or 2 per cent, supporting the view that the inner region of the boundary layer is mainly responsible for the wall pressure fluctuations.

The measurements also show that the longitudinal velocity disturbance at a particular distance from the wall, which is correlated with the wall pressure, is convected at the speed of the local mean flow.

REFERENCES

1. Allcock, G.A. et alii — *A General Purpose Analogue Computer for the Analysis of Random Noise Signals.* University of Southampton Report AASU 205, March 1962.

2. Willmarth, W.W. Woodridge, C.E. — *Measurements of the Fluctuating Pressure at the Wall Beneath a Thick Turbulent Boundary Layer.* University of Michigan Report 0290-1-T, Apr. 1962.

3. Corcos, G.M. — *Pressure Fluctuations in Shear Flows.* University of California Report, July 1962.

4. Harrison, M. — *Pressure Fluctuations on the Wall Adjacent to a Turbulent Boundary Layer.* David Taylor Model Basin Report 1260, Dec. 1958.

5. Bull, M.K. — *Space-Time Correlations of the Boundary Layer Pressure Field in Narrow Frequency Bands.* University of Southampton Report AASU 200, Dec. 1961.

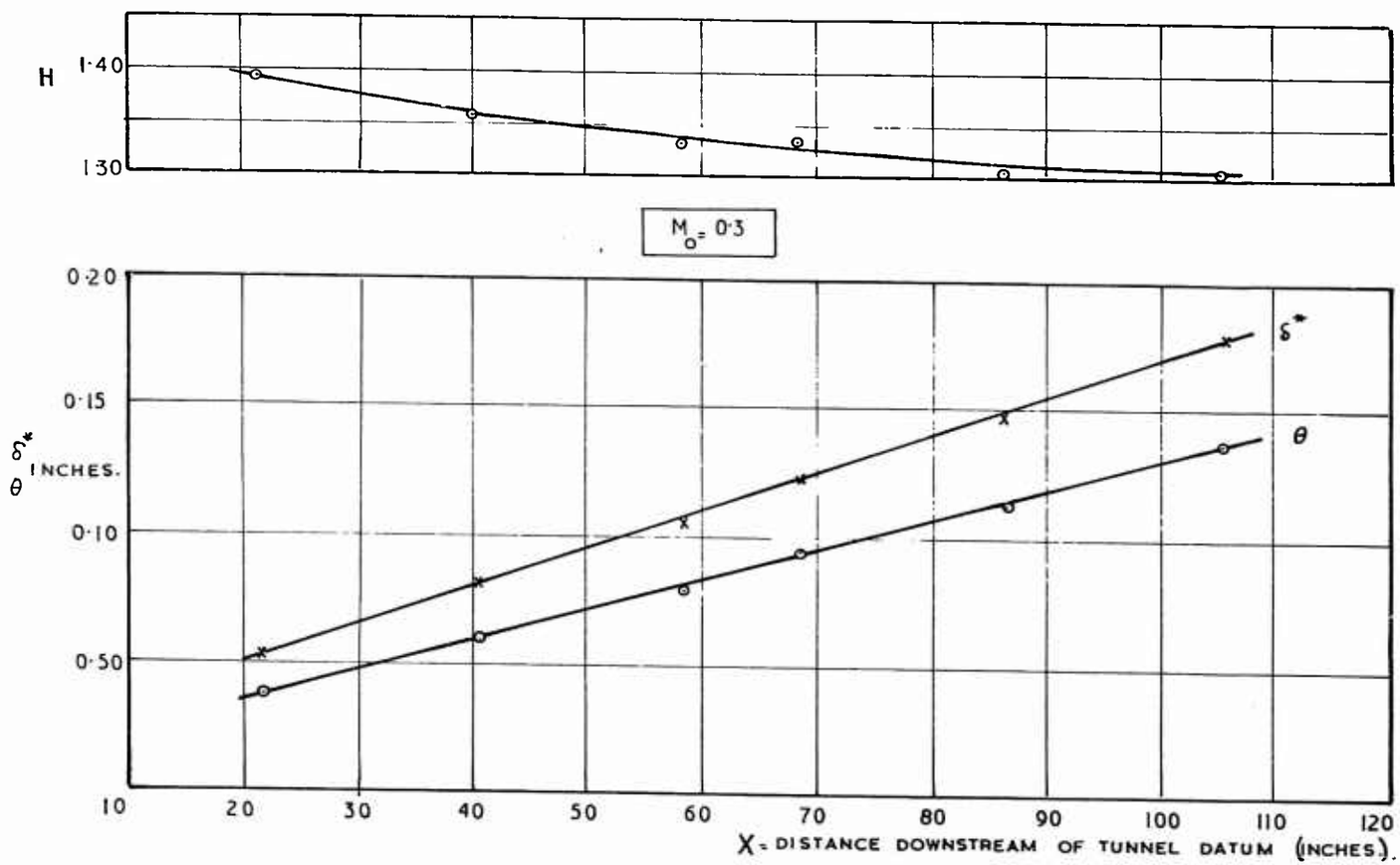

Fig.1 Variation of displacement thickness, momentum thickness and form parameter of the boundary layer, M_0 = 0.3

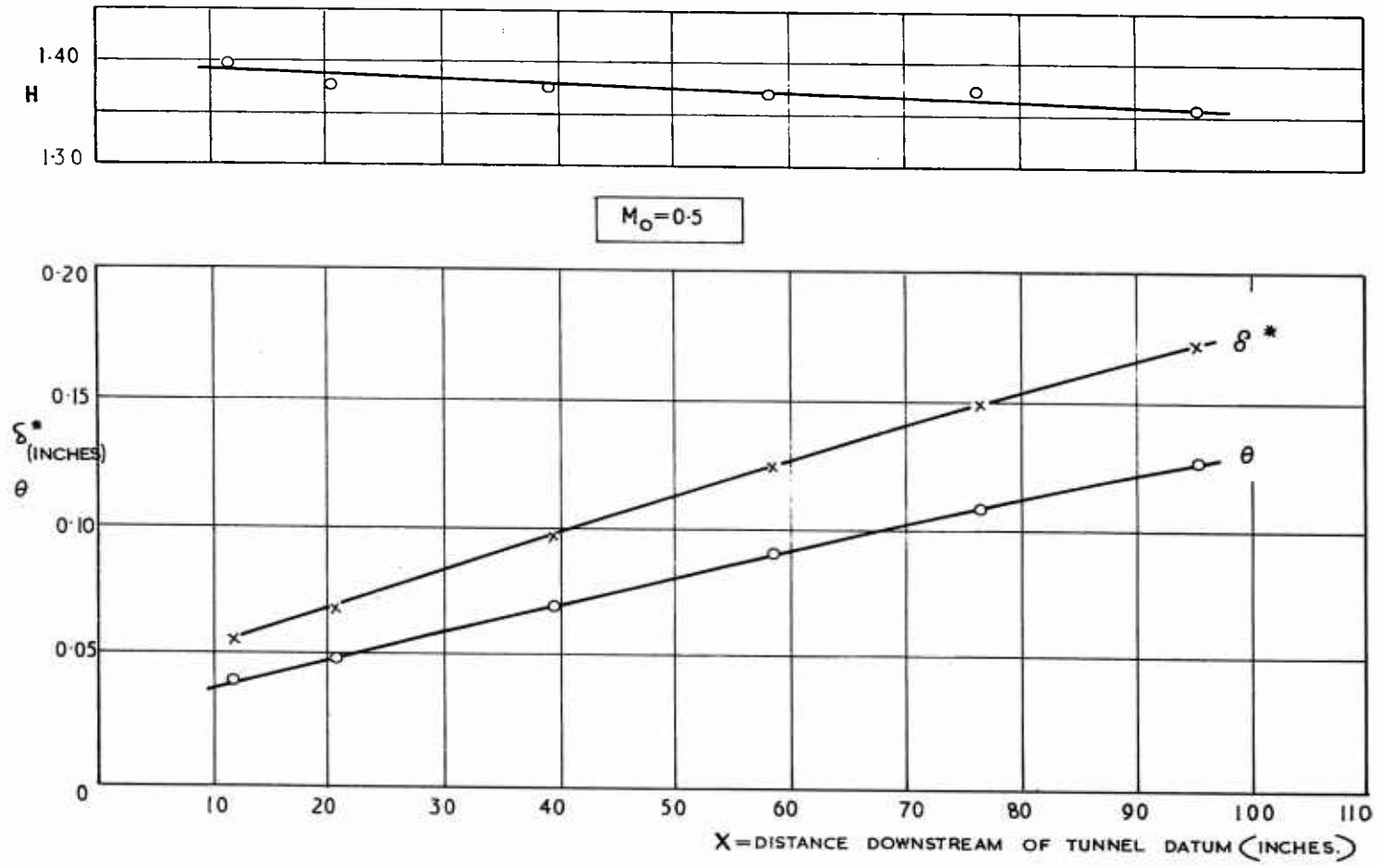

Fig. 2 Variation of displacement thickness, momentum thickness and form parameter of the boundary layer, $M_0 = 0.5$

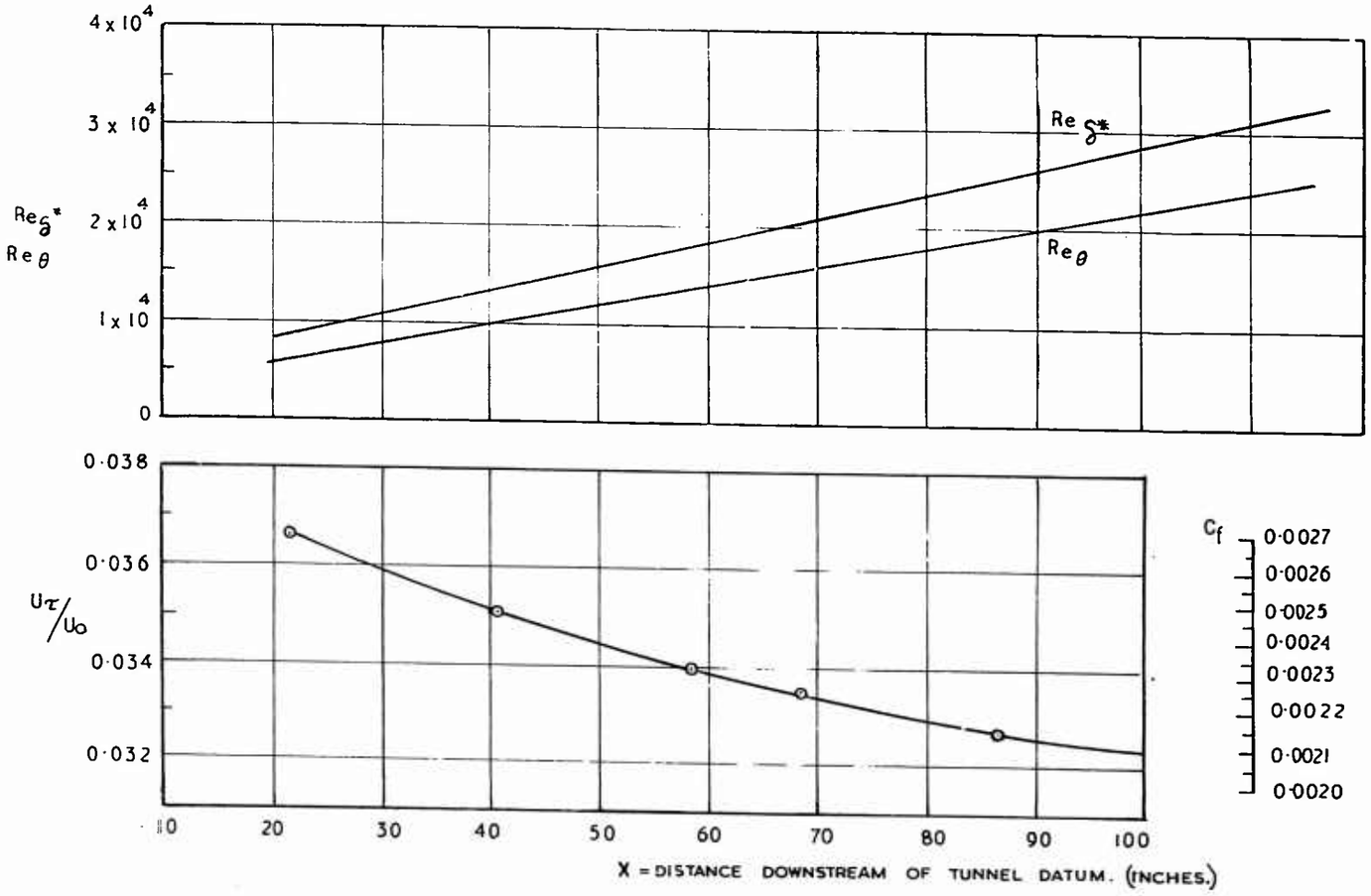

Fig. 3 Variation of Reynolds number and skin friction along the test section, $M_0 = 0.3$

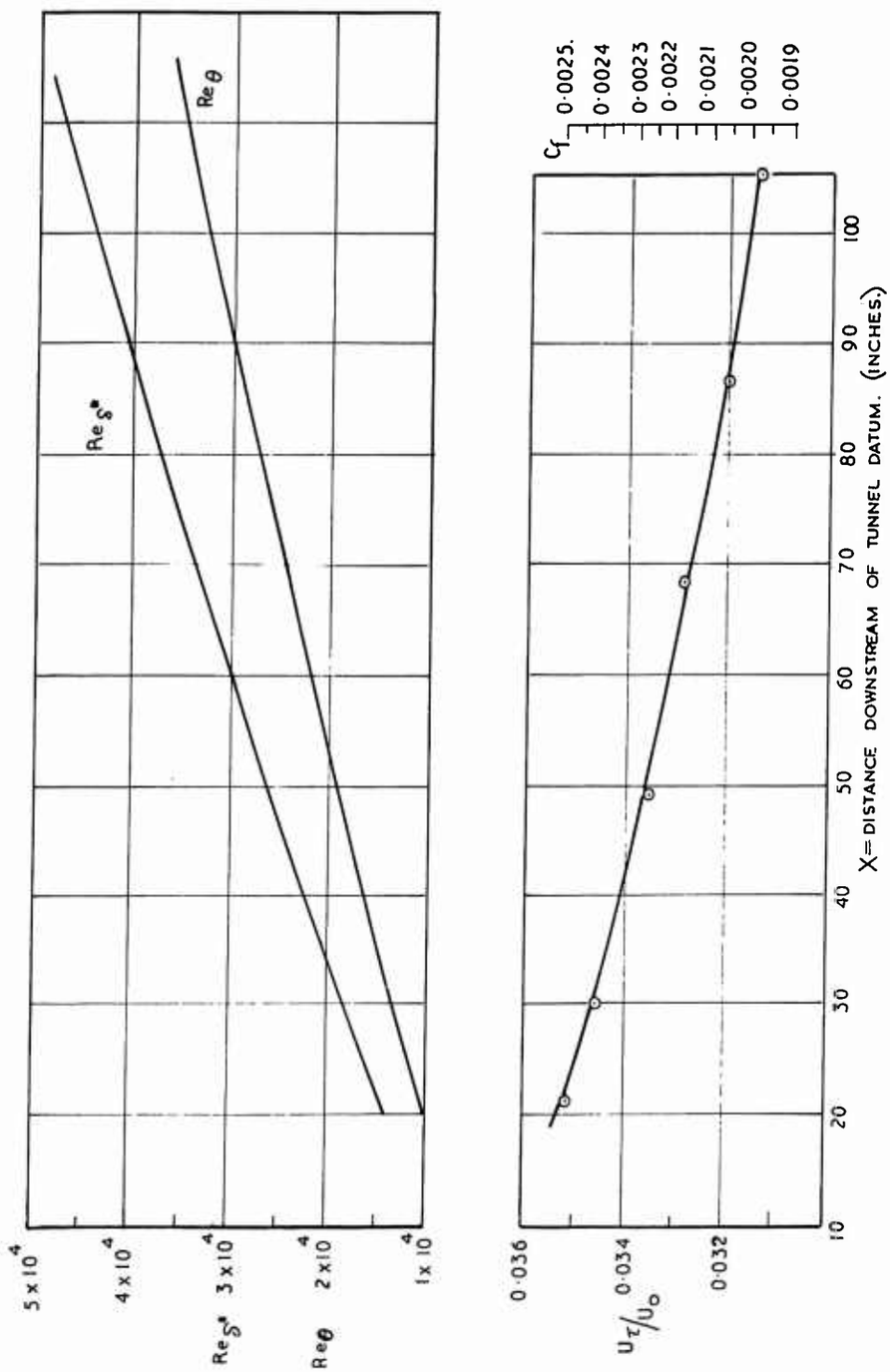

Fig. 4 Variation of Reynolds number and skin friction along the test section, $M_0 = 0.5$

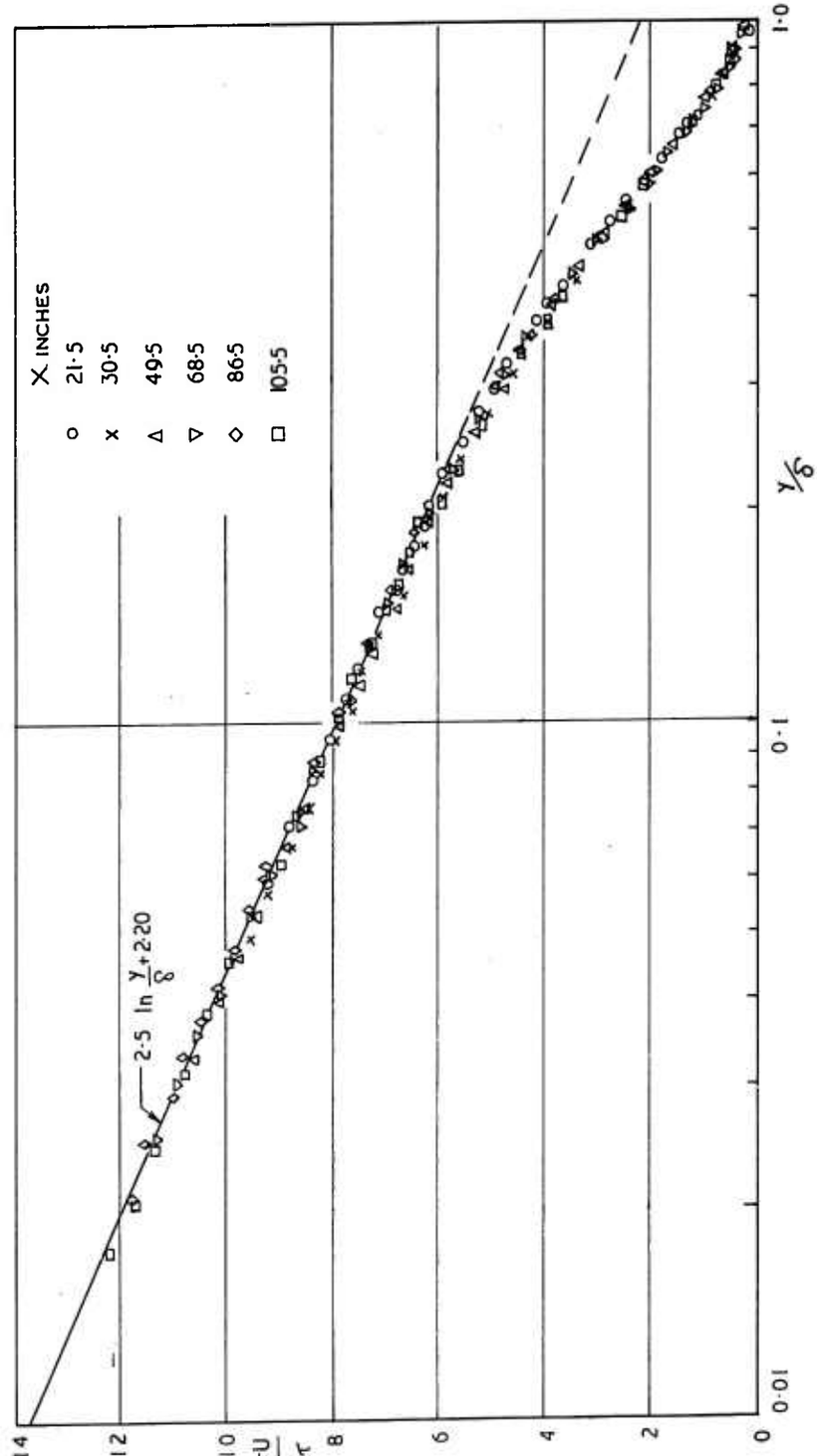

Fig.5 Boundary layer velocity profiles, $M_0 = 0.5$

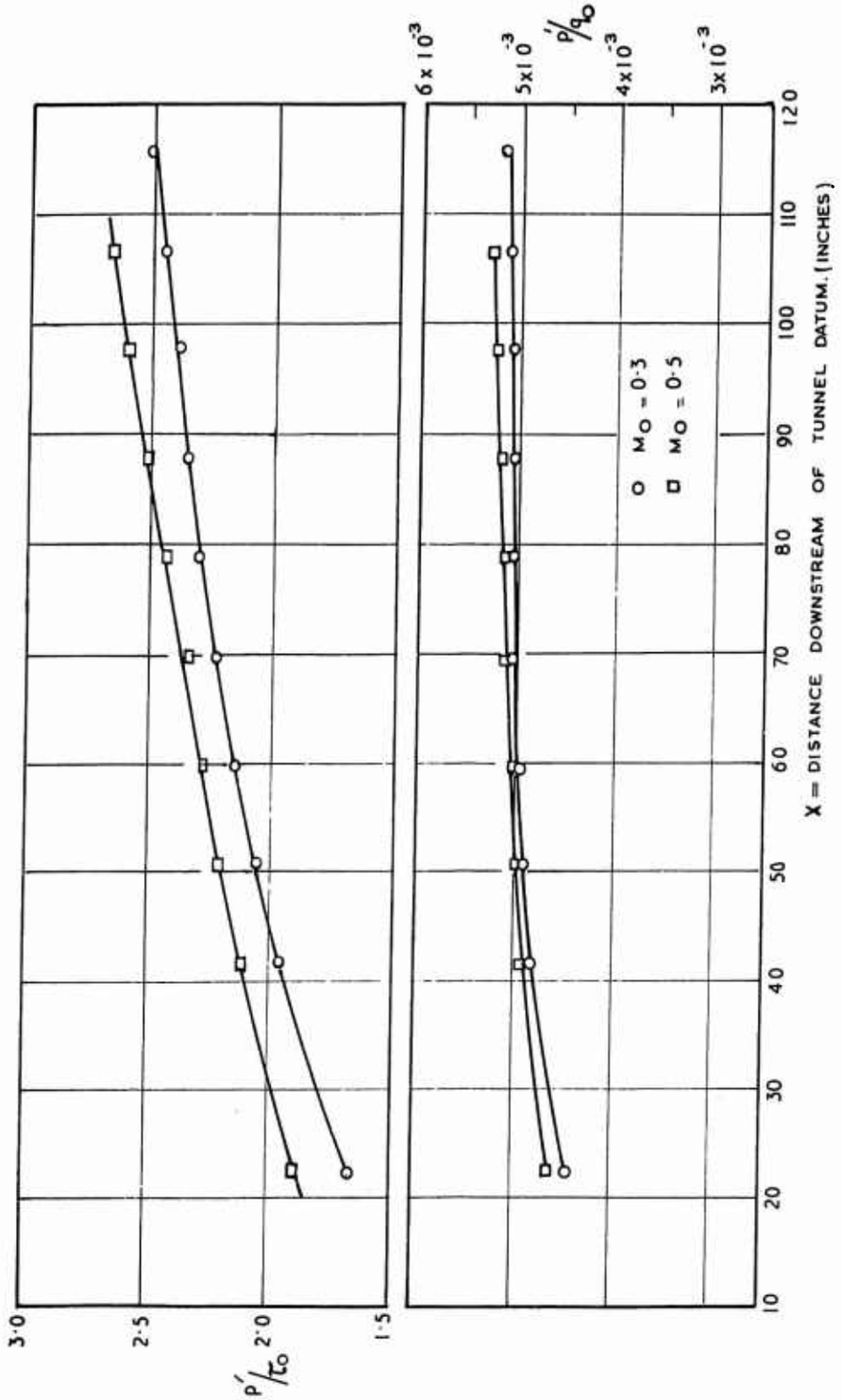

Fig.6 Variation of the rms value of wall-pressure fluctuations along the test section

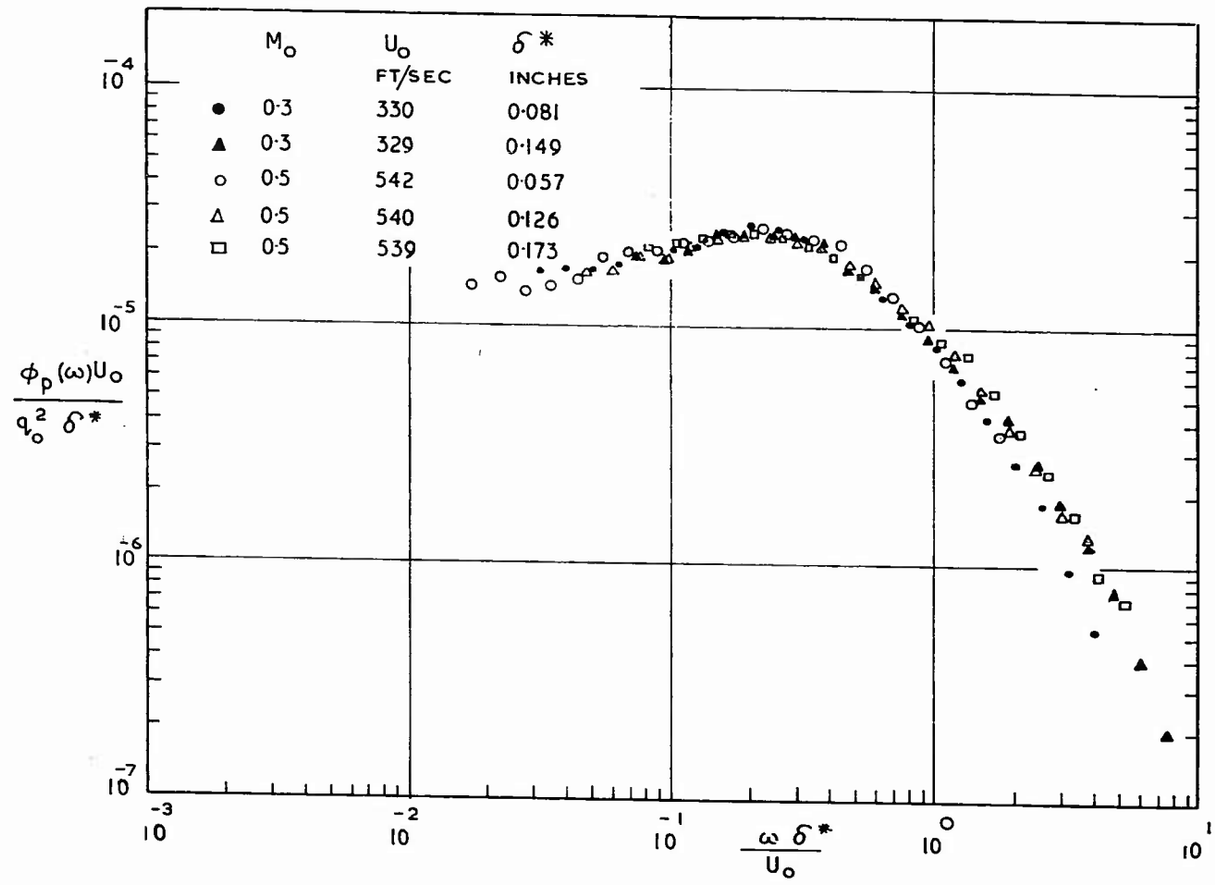

Fig.7 Frequency spectrum of wall-pressure fluctuations

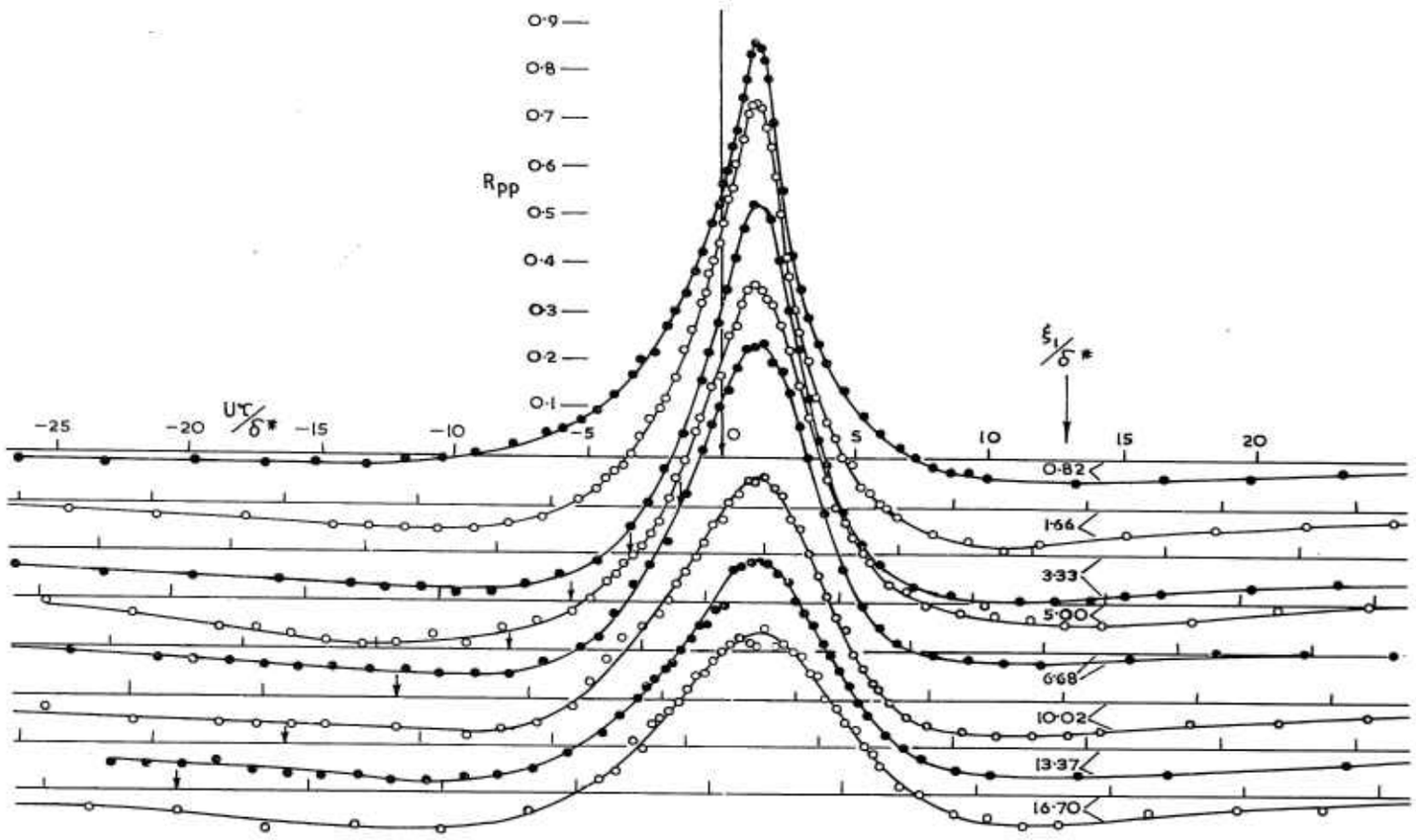

Fig. 8 Longitudinal space-time correlations of the wall-pressure field, $R_{pp}(\xi_1, 0, \tau)$
$M_0 = 0.3$, $\delta^* = 0.149$ inches, X = 87.6 inches
(arrows indicate locations of origins)

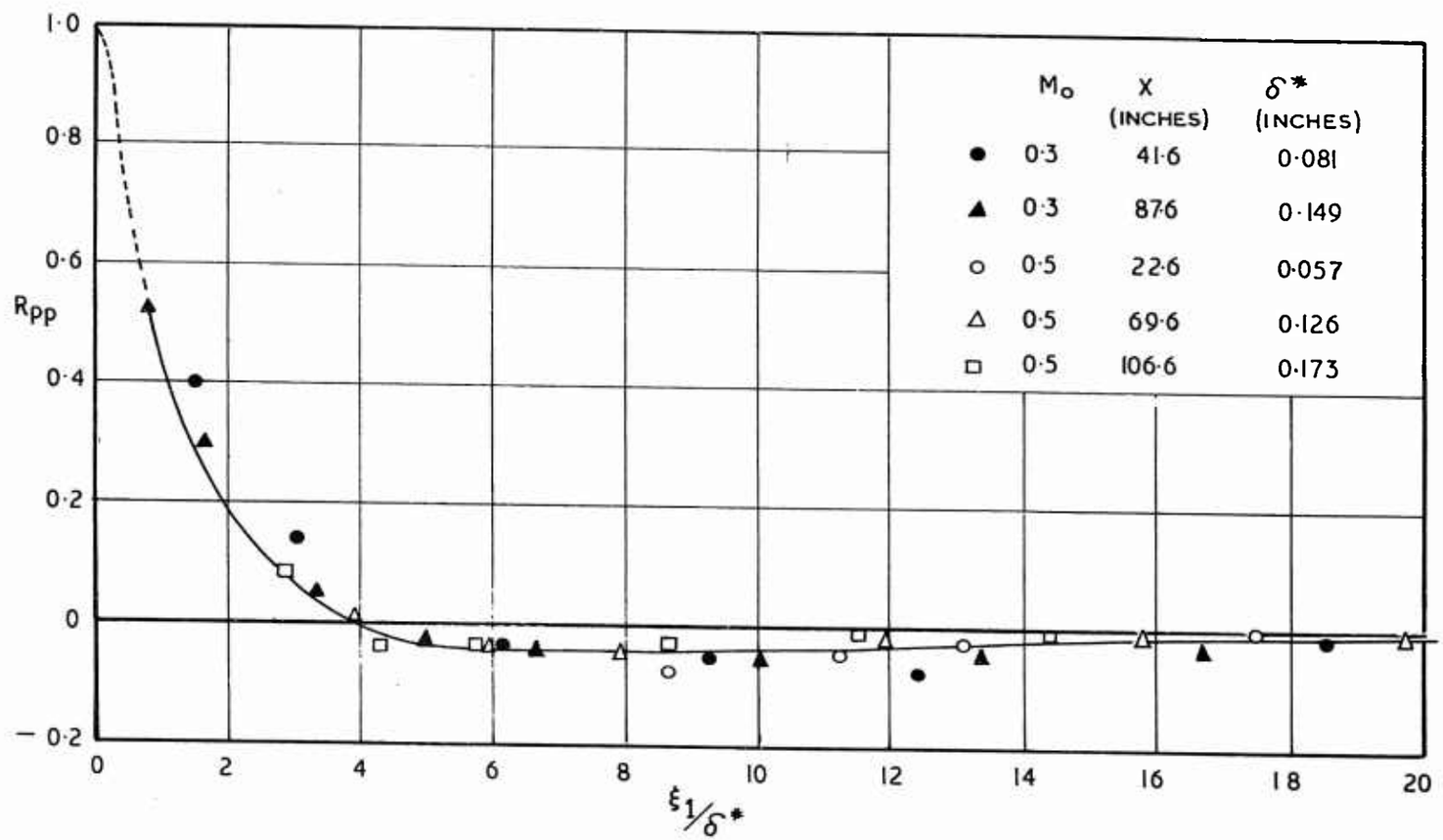

Fig. 9 Longitudinal space correlation of the wall-pressure field, $R_{pp}(\xi_1, 0, 0)$

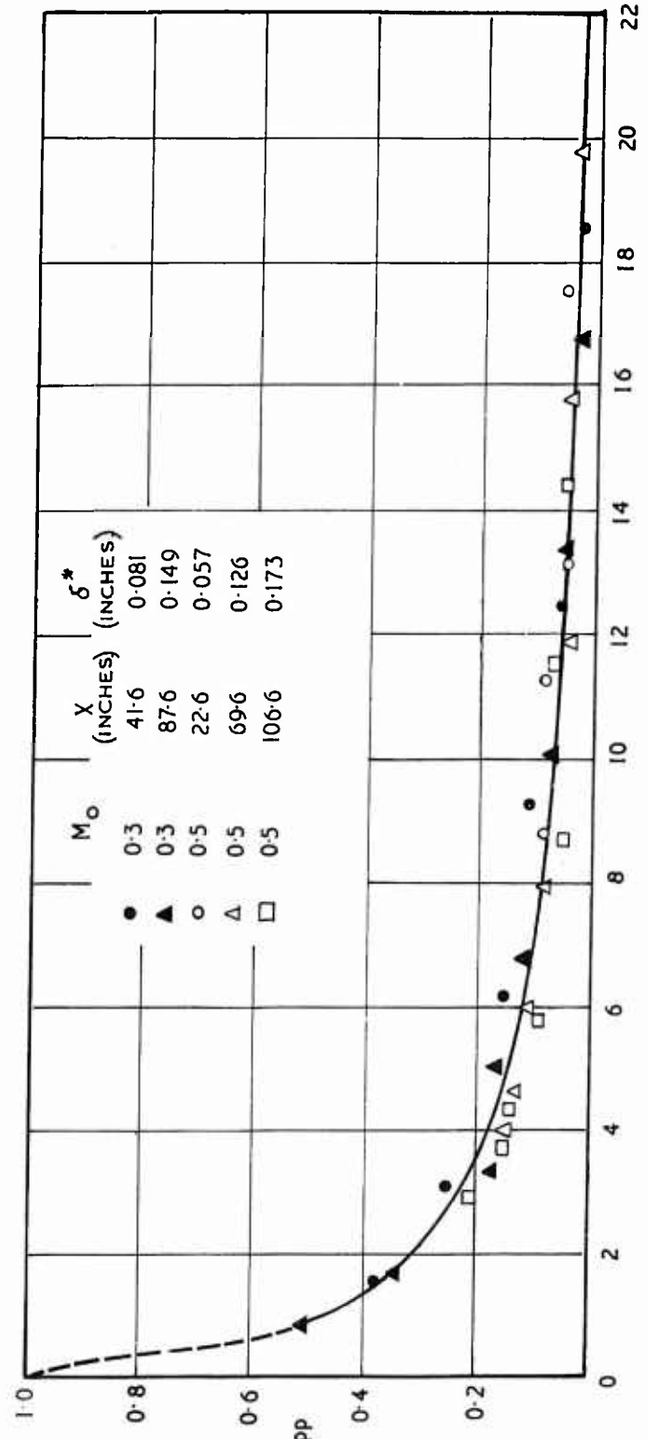

Fig. 10 Lateral space correlation of the wall-pressure field, $R_{pp}(0,\xi_3,0)$

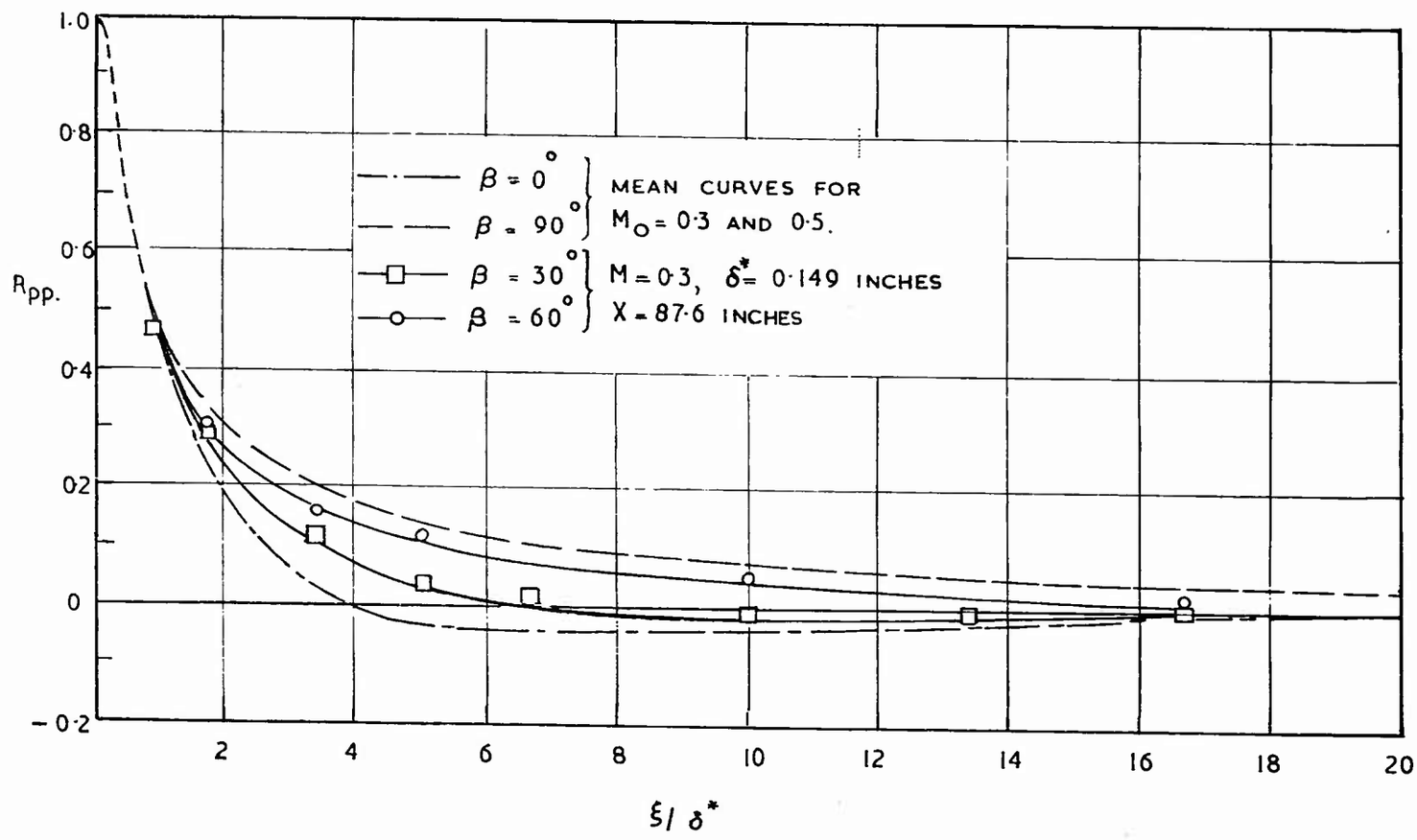

Fig. 11 Space correlations of the wall-pressure field, $R_{pp}(\xi\cos\theta, \xi\sin\theta, 0)$, at various angles to the flow direction

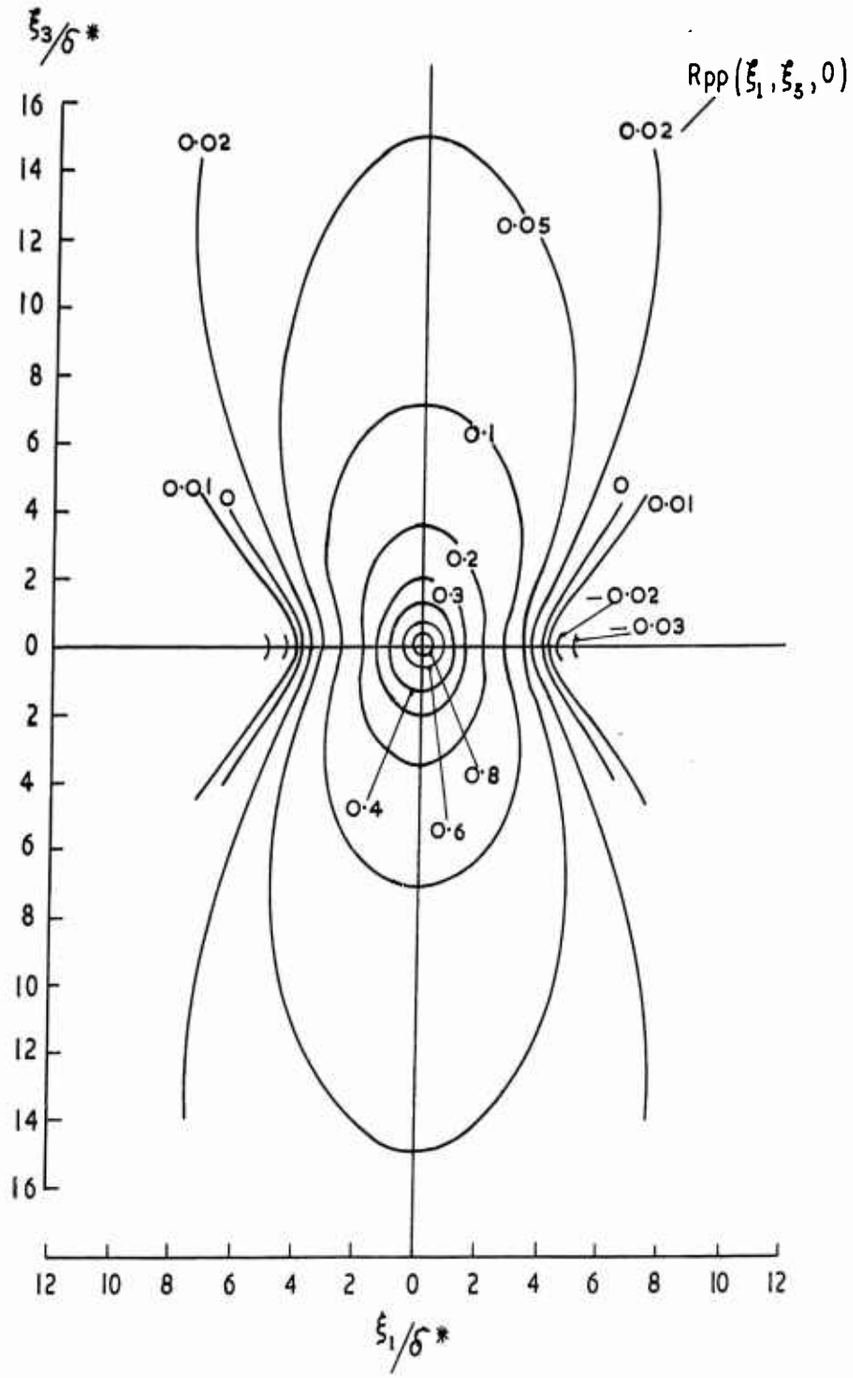

Fig. 12 Contours of constant space correlation, $R_{pp}(\xi_1, \xi_3, 0)$, of the wall-pressure field

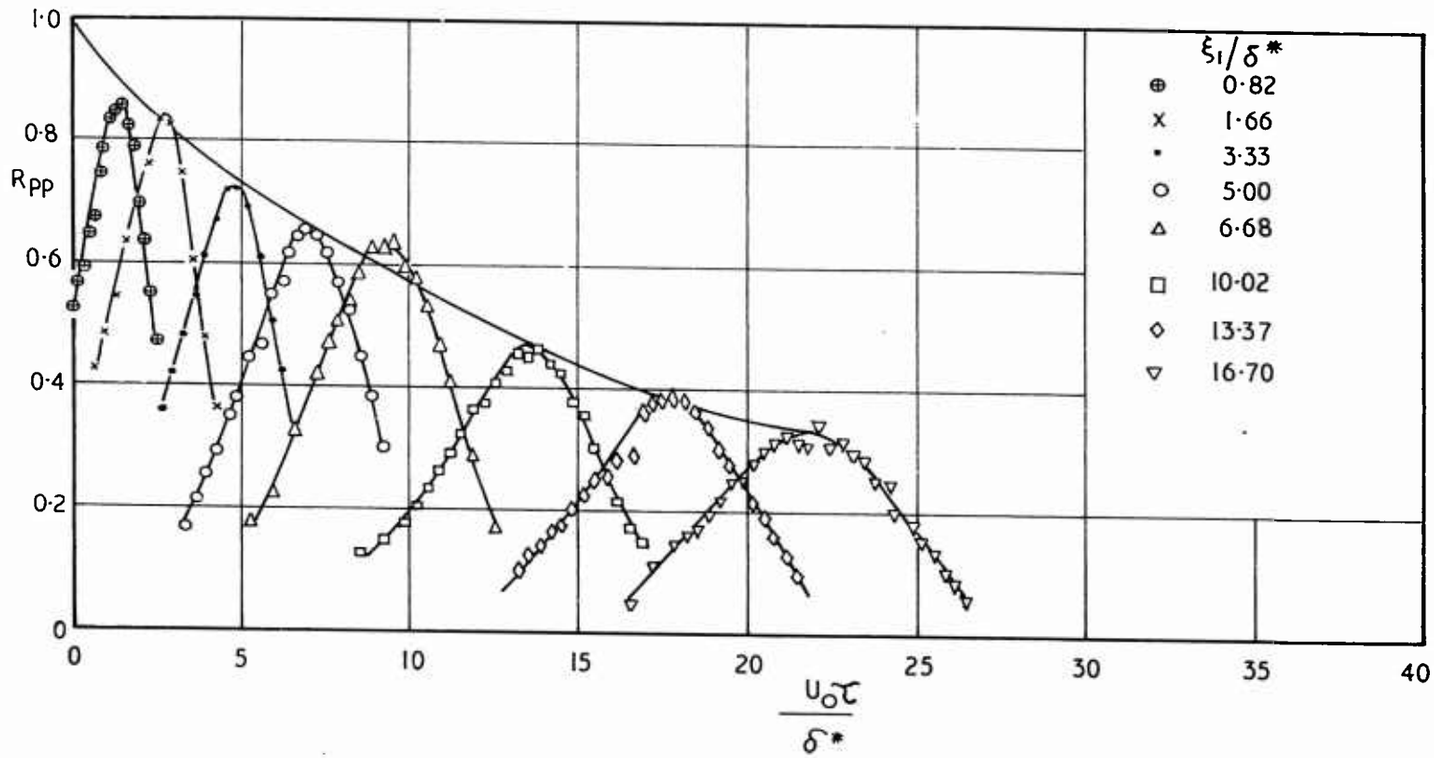

Fig. 13 Peaks of curves of longitudinal space-time correlation, $R_{pp}(\xi_1, 0, \tau)$
$M_0 = 0.3$, $\delta^* = 0.149$ inch, X = 87.6 inches

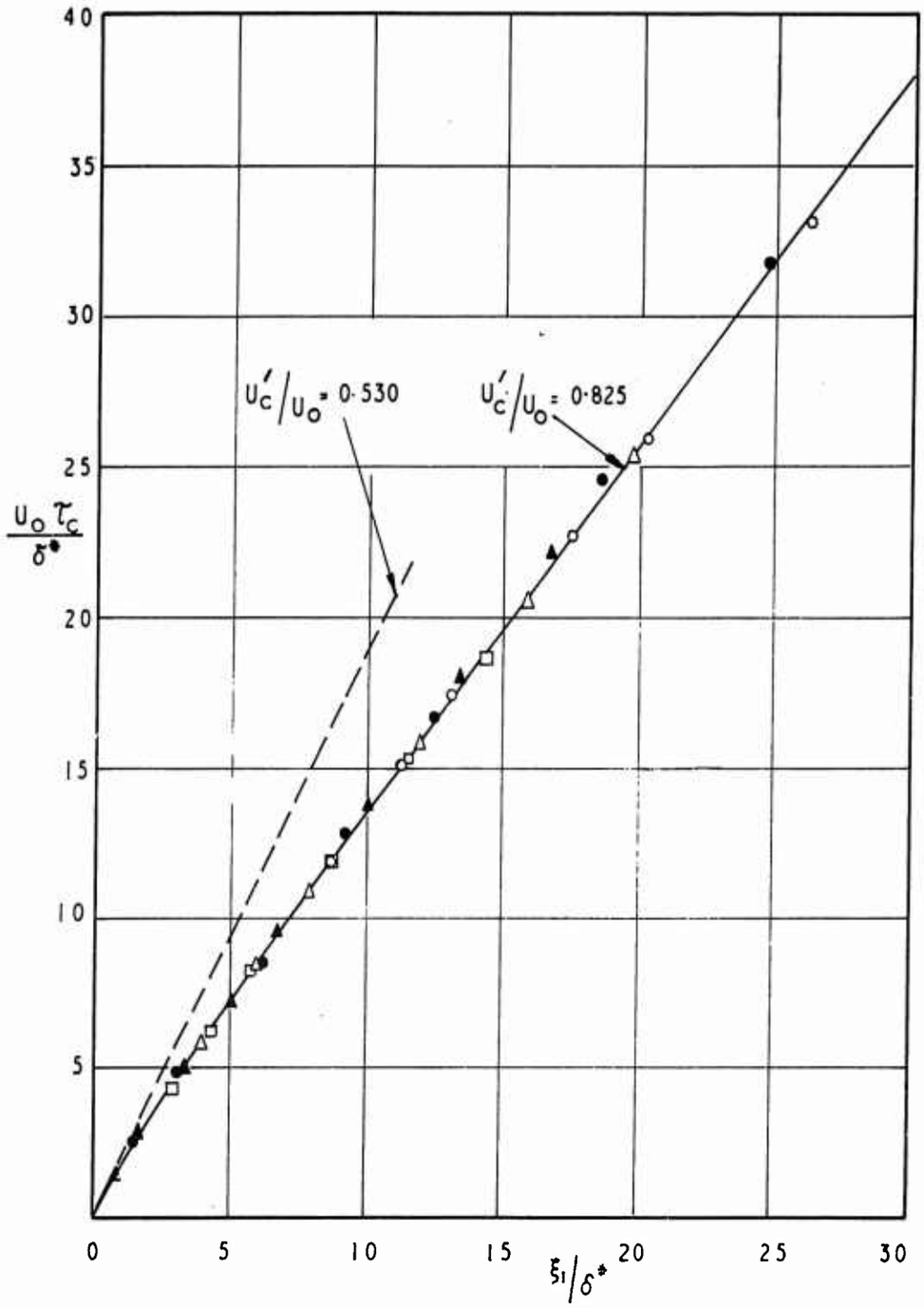

Fig. 14 Variation of convection time with spatial separation

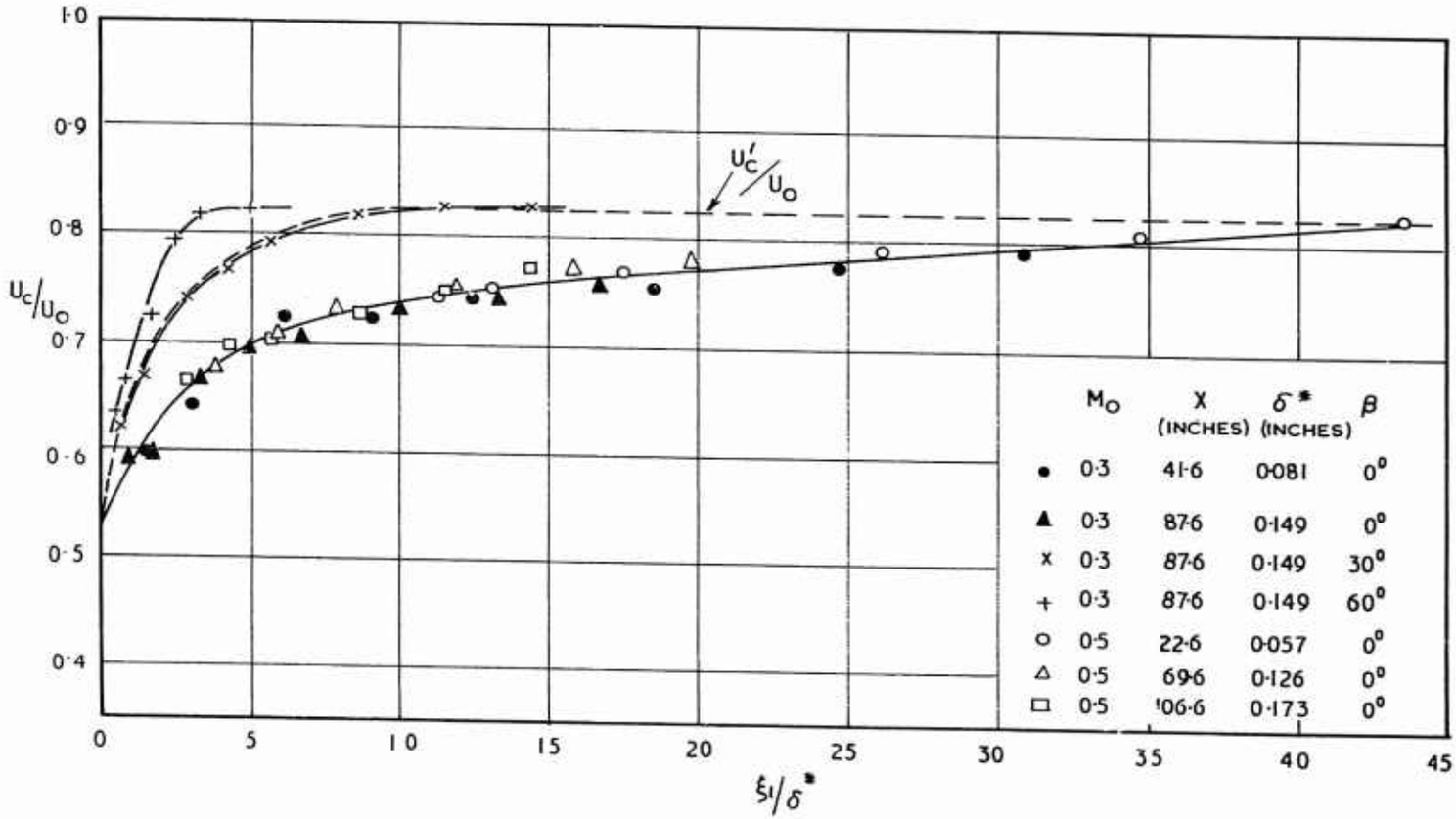

Fig. 15 Variation of convection velocity with spatial separation

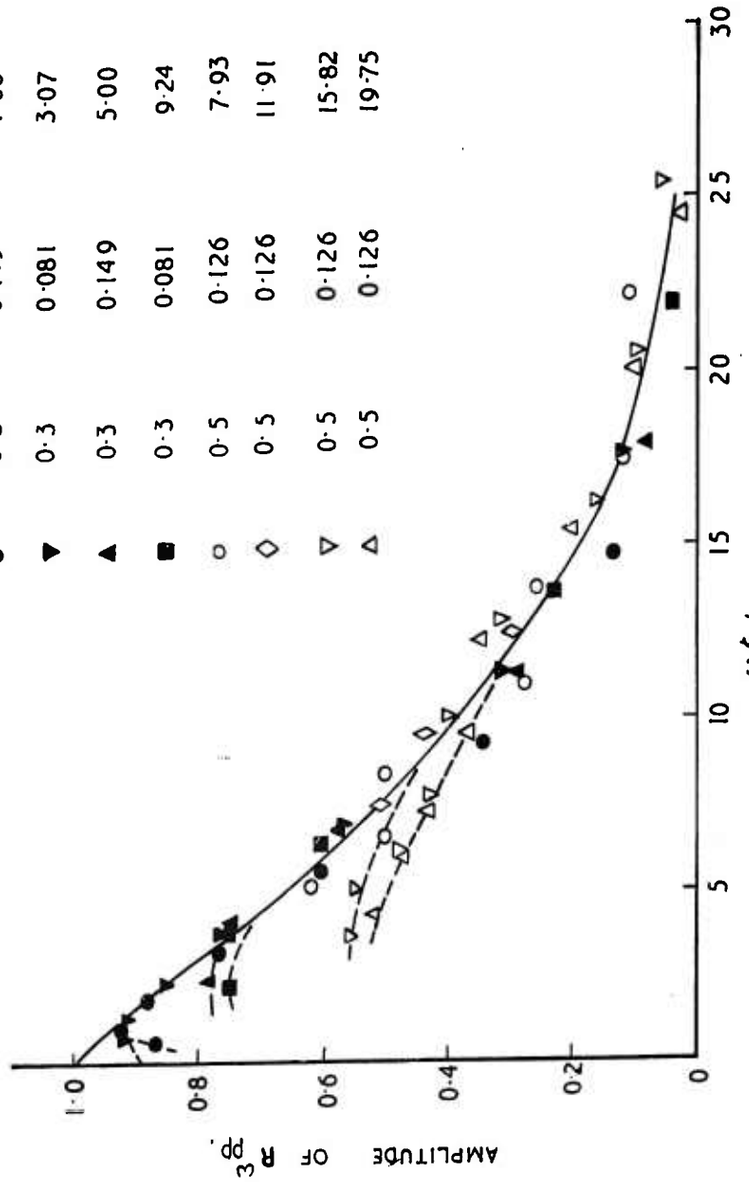

Fig. 16 Amplitude of narrow-band longitudinal space-time correlations of the wall-pressure field

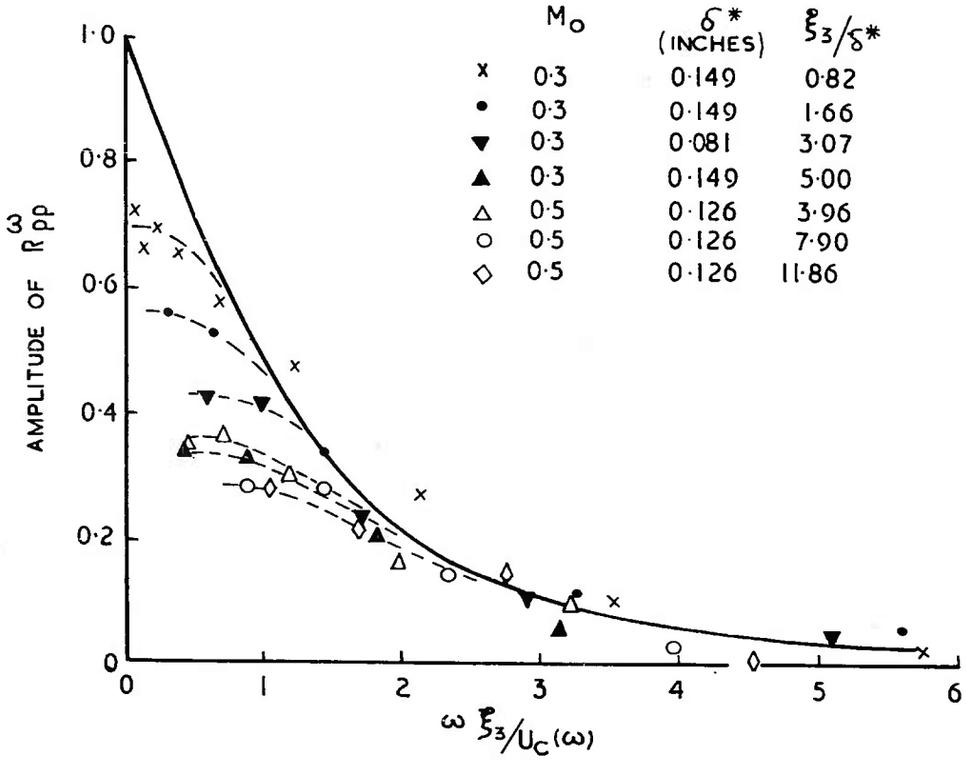

Fig. 17 Amplitude of narrow-band lateral space-time correlation of the wall-pressure field

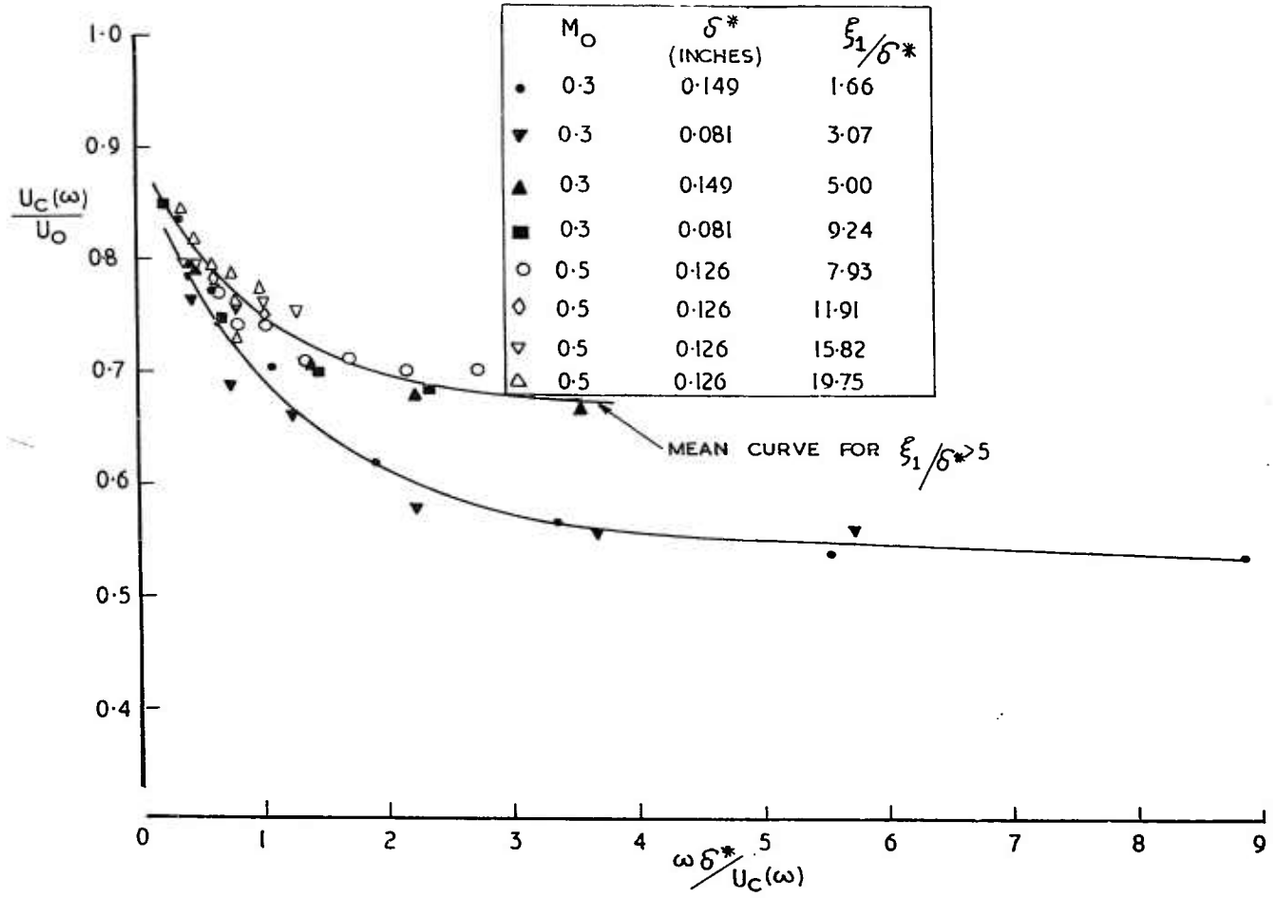

Fig. 18 Convection velocities of the wall-pressure field from narrow-band measurements

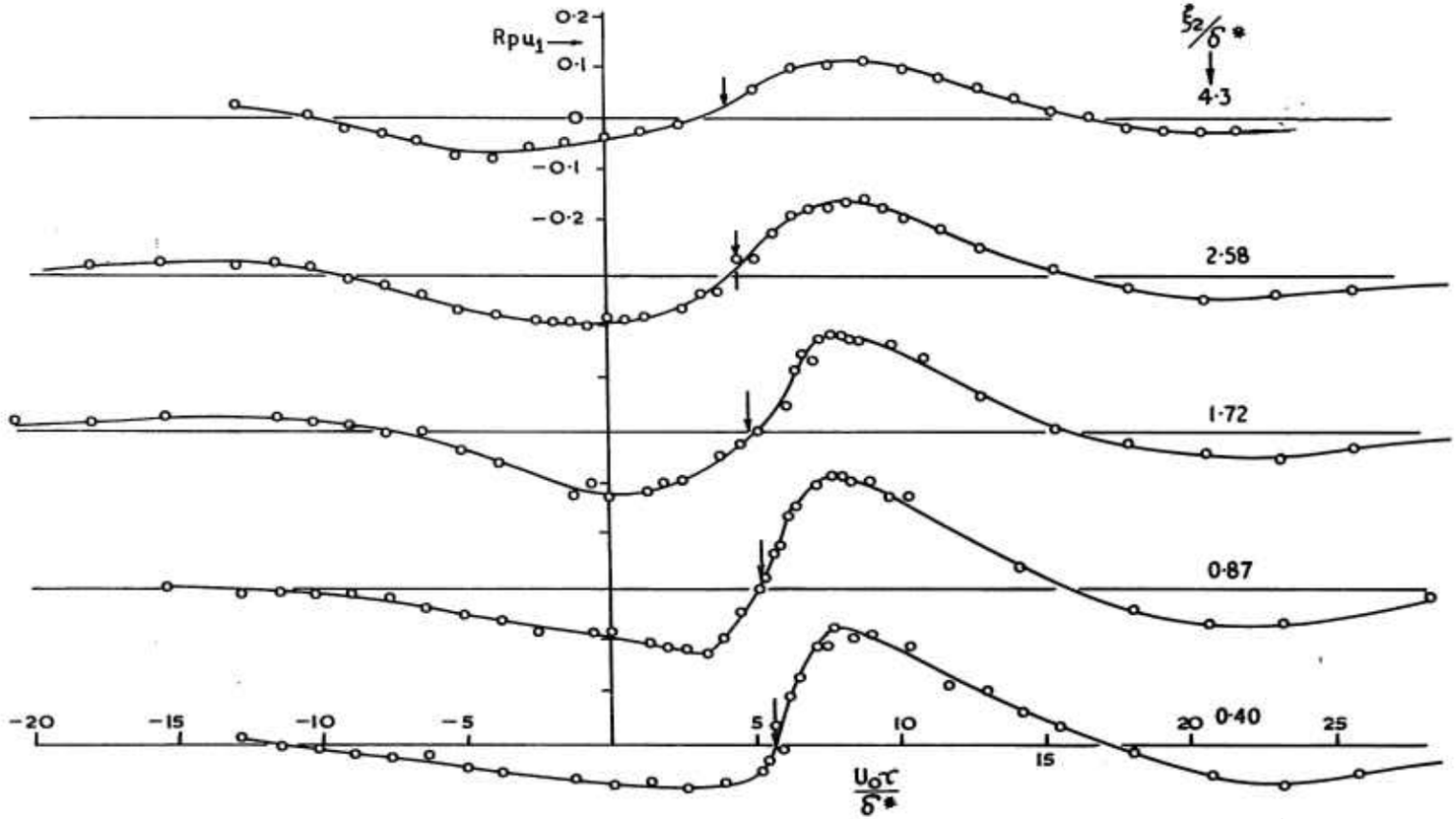

Fig. 19 Space-time correlations of the wall-pressure and longitudinal velocity component $R_{pu_1}(\xi_1,\xi_2,0,\tau)$; $M_0 = 0.5$; $\delta^* = 0.126$ inches; X = 69.6 inches (arrows show time delay corresponding to local mean velocity)

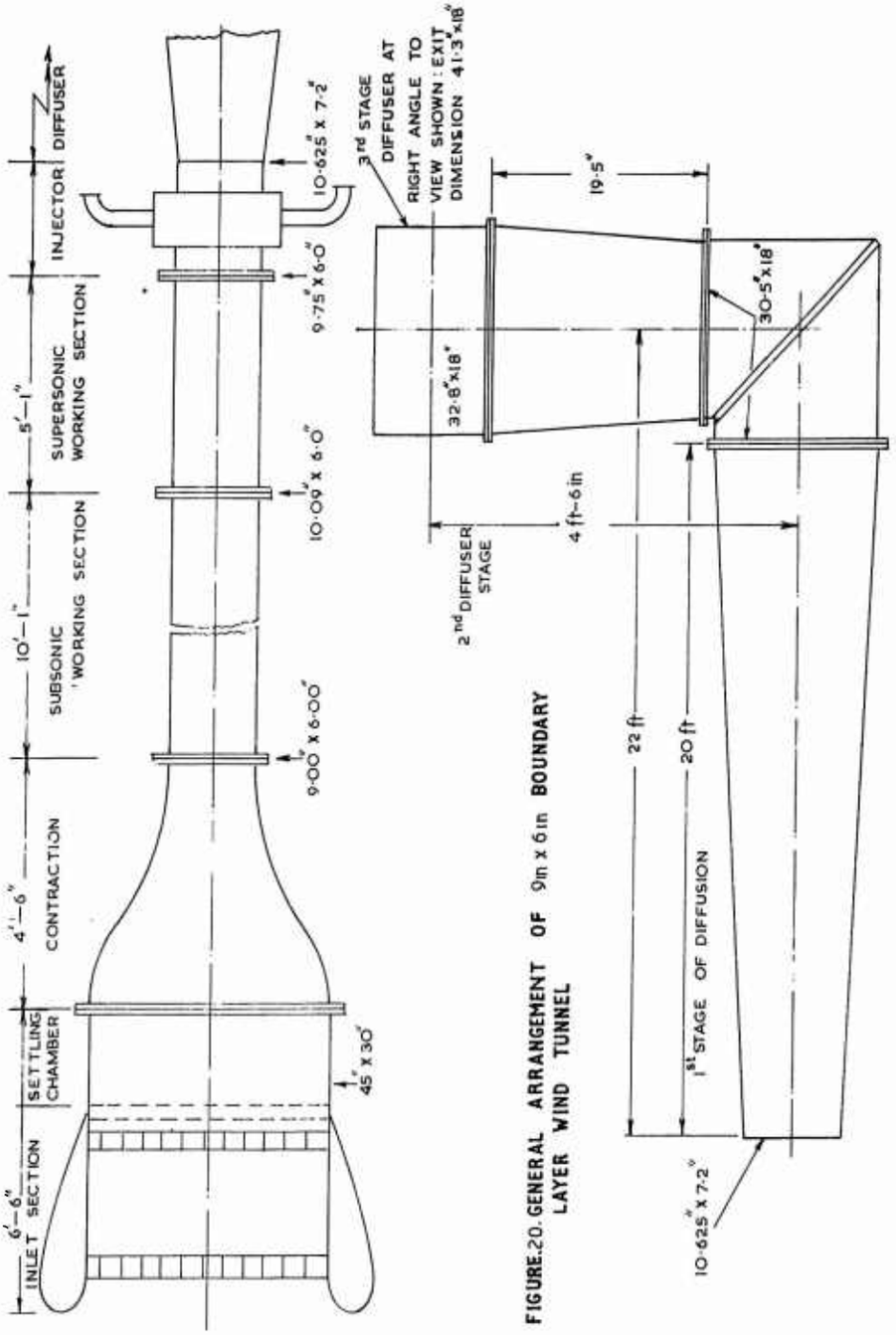

FIGURE.20. GENERAL ARRANGEMENT OF 9m x 6in BOUNDARY LAYER WIND TUNNEL

Fig. 20 General arrangement of 9 in × 6 in boundary layer wind tunnel

DISCUSSION

Comment by P. Davies

Dr. Curle of Southampton has investigated the effect of discarding parts of a flat spectrum and shows the error of doing so is not large. This is not of course true when discrete frequencies form a large proportion of the overall signal power.

Comment by J.S. Serafini

I would like to clarify and emphasize the points I made after the paper by W.W. Willmarth. Of importance in the filtering here is not only what is the cut-off frequency, but how sharply the rate of cut-off takes place. What is your rate of cut-off of your filter, Dr. Bull?

Author's reply

In obtaining the pressure-velocity correlations the low-frequency cut-off for $\omega\delta^*/V_0 < 0.14$ was sharp, from memory 12 db/octave .

Comment by J.S. Serafini

If indeed your cut-off is quite sharp, note that in so doing you have removed not just increased spectral level due to interference, but you also have removed the 'non-interfered' level in this filtered range of the frequency. Thus, it is not entirely clear to me precisely under what grounds one can neglect the fact that in removing the 'interference effect' by sharply filtering the spectra one also has changed the basic character of the fluctuations to be correlated.

Author's reply

It is true that filtering removed the true signal as well as the interference effect but the contribution to the pressure energy from frequencies for which $\omega\delta^*/U_0 < 0.14$ amounts to only 3 or 4 per cent of the total, and I believe that the effect on the measured correlations is small.

M. Strasberg

Dr. Serafini's point, that the contribution of the low frequencies to the cross correlation may be greater than their contribution to the mean-square signal itself, is well taken. This may be stated in a more definite way be noting that the cross correlation is the Fourier transform of the spectral density, viz.

$$R_{12}(T) = \frac{1}{\pi}\int_0^\infty \left[P_{12}(\omega)\cos\omega T + Q_{12}(\omega)\sin\omega T \right] d\omega$$

where P_{12} and Q_{12} are the real and imaginary parts of the cross-spectral density. If the signals are filtered with high-pass filters having a cut-off frequency ω_c ,

then the integration is performed only from ω_c to ∞. But the contribution to the integral of P_{12} and Q_{12} from zero to ω_c may be a larger portion of the total integral than the contribution of $P_{11}(\omega)$ to the mean-square signal.

Author's reply

Errors could certainly be introduced in this way, but it was found that when the interference effect itself was small, the effect of filtering was also small, producing changes in correlation coefficient of the order of 0.01 or 0.02 when the interference signal produced about 2 per cent increase of rms pressure - only in the case of large interference effects did filtering give rise to large changes in correlation coefficient. This reinforces my belief that the effect of filtering in this case has been to remove the interference signal without significantly affecting the correlation of the real pressure signal with the velocity.

DISTRIBUTION

Copies of AGARD publications may be obtained in the various countries at the addresses given below.

On peut se procurer des exemplaires des publications de l'AGARD aux adresses suivantes.

BELGIUM BELGIQUE	Centre National d'Etudes et de Recherches Aéronautiques 11, rue d'Egmont, Bruxelles
CANADA	Director of Scientific Information Service Defense Research Board Department of National Defense 'A' Building, Ottawa, Ontario
DENMARK DANEMARK	Military Research Board Defense Staff Kastellet, Copenhagen Ø
FRANCE	O.N.E.R.A. (Direction) 25, Avenue de la Division Leclerc Châtillon-sous-Bagneux (Seine)
GERMANY ALLEMAGNE	Wissenschaftliche Gesellschaft für Luftfahrt Zentralstelle der Luftfahrtdokumentation Munchen 64, Flughafen Attn: Dr. H.J. Rautenberg
GREECE GRECE	Greek National Defense General Staff B. MEO Athens
ICELAND ISLANDE	Director of Aviation c/o Flugrad Reykjavik
ITALY ITALIE	Ufficio del Generale Ispettore del Genio Aeronautico Ministero Difesa Aeronautica Roma
LUXEMBURG LUXEMBOURG	Obtainable through Belgium
NETHERLANDS PAYS BAS	Netherlands Delegation to AGARD Michiel de Ruyterweg 10 Delft

NORWAY NORVEGE	Mr. O. Blichner Norwegian Defence Research Establishment Kjeller per Lillestrom
PORTUGAL	Col. J.A. de Almeida Viama (Delegado Nacional do 'AGARD') Direcção do Serviço de Material da F.A. Rua da Escola Politecnica, 42 Lisboa
TURKEY TURQUIE	Ministry of National Defence Ankara Attn. AGARD National Delegate
UNITED KINGDOM ROYAUME UNI	Ministry of Aviation T.I.L., Room 009A First Avenue House High Holborn London W.C.1
UNITED STATES ETATS UNIS	National Aeronautics and Space Administration (NASA) 1520 H Street, N.W. Washington 25, D.C.

Printed by Technical Editing and Reproduction Ltd
Harford House, 7-9 Charlotte St. London. W.1.

AGARD Report 455	532.526.4 3b2f:3b2e1a
North Atlantic Treaty Organization, Advisory Group for Aeronautical Research and Development PROPERTIES OF THE FLUCTUATING WALL-PRESSURE FIELD OF A TURBULENT BOUNDARY LAYER M.K. Bull 1963 34 pp., incl. 5 refs., 20 figs & discussion The results of measurements of various statistical properties of the fluctuating wall-pressure field associated with turbulent subsonic boundary layer flow in conditions covering a range of values of boundary layer thickness and flow speed are given. The measured quantities include overall rms pressures, frequency spectra, and longitudinal and P.T.O.	

AGARD Report 455
North Atlantic Treaty Organization, Advisory Group for Aeronautical Research and Development
PROPERTIES OF THE FLUCTUATING WALL-PRESSURE FIELD OF A TURBULENT BOUNDARY LAYER
M.K. Bull
1963
34 pp., incl. 5 refs., 20 figs & discussion

The results of measurements of various statistical properties of the fluctuating wall-pressure field associated with turbulent subsonic boundary layer flow in conditions covering a range of values of boundary layer thickness and flow speed are given. The measured quantities include overall rms pressures, frequency spectra, and longitudinal and

P.T.O.

532.526.4
3b2f:3b2e1a

AGARD Report 455
North Atlantic Treaty Organization, Advisory Group for Aeronautical Research and Development
PROPERTIES OF THE FLUCTUATING WALL-PRESSURE FIELD OF A TURBULENT BOUNDARY LAYER
M.K. Bull
1963
34 pp., incl. 5 refs., 20 figs & discussion

The results of measurements of various statistical properties of the fluctuating wall-pressure field associated with turbulent subsonic boundary layer flow in conditions covering a range of values of boundary layer thickness and flow speed are given. The measured quantities include overall rms pressures, frequency spectra, and longitudinal and

P.T.O.

532.526.4
3b2f:3b2e1a

AGARD Report 455
North Atlantic Treaty Organization, Advisory Group for Aeronautical Research and Development
PROPERTIES OF THE FLUCTUATING WALL-PRESSURE FIELD OF A TURBULENT BOUNDARY LAYER
M.K. Bull
1963
34 pp., incl. 5 refs., 20 figs & discussion

The results of measurements of various statistical properties of the fluctuating wall-pressure field associated with turbulent subsonic boundary layer flow in conditions covering a range of values of boundary layer thickness and flow speed are given. The measured quantities include overall rms pressures, frequency spectra, and longitudinal and

P.T.O.

532.526.4
3b2f:3b2e1a

lateral space-time correlations in both broad and narrow frequency bands. Some experimental values of space-time correlation between wall-pressure fluctuations and turbulent velocity fluctuations at various positions in the boundary layer are also presented.

These experimental results and some of their implications on the structure of the wall-pressure field and the nature of its convection and decay are discussed.

This Report is one in the Series 448-469 inclusive, presenting papers, with discussions, given at the AGARD Specialists' Meeting on 'The Mechanism of Noise Generation in Turbulent Flow' at the Training Center for Experimental Aerodynamics, Rhode-Saint-Genèse, Belgium, 1-5 April 1963, sponsored by the AGARD Fluid Dynamics Panel.

lateral space-time correlations in both broad and narrow frequency bands. Some experimental values of space-time correlation between wall-pressure fluctuations and turbulent velocity fluctuations at various positions in the boundary layer are also presented.

These experimental results and some of their implications on the structure of the wall-pressure field and the nature of its convection and decay are discussed.

This Report is one in the Series 448-469 inclusive, presenting papers, with discussions, given at the AGARD Specialists' Meeting on 'The Mechanism of Noise Generation in Turbulent Flow' at the Training Center for Experimental Aerodynamics, Rhode-Saint-Genèse, Belgium, 1-5 April 1963, sponsored by the AGARD Fluid Dynamics Panel.

lateral space-time correlations in both broad and narrow frequency bands. Some experimental values of space-time correlation between wall-pressure fluctuations and turbulent velocity fluctuations at various positions in the boundary layer are also presented.

These experimental results and some of their implications on the structure of the wall-pressure field and the nature of its convection and decay are discussed.

This Report is one in the Series 448-469 inclusive, presenting papers, with discussions, given at the AGARD Specialists' Meeting on 'The Mechanism of Noise Generation in Turbulent Flow' at the Training Center for Experimental Aerodynamics, Rhode-Saint-Genèse, Belgium, 1-5 April 1963, sponsored by the AGARD Fluid Dynamics Panel.

lateral space-time correlations in both broad and narrow frequency bands. Some experimental values of space-time correlation between wall-pressure fluctuations and turbulent velocity fluctuations at various positions in the boundary layer are also presented.

These experimental results and some of their implications on the structure of the wall-pressure field and the nature of its convection and decay are discussed.

This Report is one in the Series 448-469 inclusive, presenting papers, with discussions, given at the AGARD Specialists' Meeting on 'The Mechanism of Noise Generation in Turbulent Flow' at the Training Center for Experimental Aerodynamics, Rhode-Saint-Genèse, Belgium, 1-5 April 1963, sponsored by the AGARD Fluid Dynamics Panel.

AGARD Report 455
North Atlantic Treaty Organization, Advisory Group for Aeronautical Research and Development
PROPERTIES OF THE FLUCTUATING WALL-PRESSURE FIELD OF A TURBULENT BOUNDARY LAYER
M.K. Bull
1963
34 pp., incl. 5 refs., 20 figs & discussion

532.526.4
3b2f:3b2e1a

The results of measurements of various statistical properties of the fluctuating wall-pressure field associated with turbulent subsonic boundary layer flow in conditions covering a range of values of boundary layer thickness and flow speed are given. The measured quantities include overall rms pressures, frequency spectra, and longitudinal and

P.T.O.

AGARD Report 455
North Atlantic Treaty Organization, Advisory Group for Aeronautical Research and Development
PROPERTIES OF THE FLUCTUATING WALL-PRESSURE FIELD OF A TURBULENT BOUNDARY LAYER
M.K. Bull
1963
34 pp., incl. 5 refs., 20 figs & discussion

532.526.4
3b2f:3b2e1a

The results of measurements of various statistical properties of the fluctuating wall-pressure field associated with turbulent subsonic boundary layer flow in conditions covering a range of values of boundary layer thickness and flow speed are given. The measured quantities include overall rms pressures, frequency spectra, and longitudinal and

P.T.O.

AGARD Report 455
North Atlantic Treaty Organization, Advisory Group for Aeronautical Research and Development
PROPERTIES OF THE FLUCTUATING WALL-PRESSURE FIELD OF A TURBULENT BOUNDARY LAYER
M.K. Bull
1963
34 pp., incl. 5 refs., 20 figs & discussion

532.526.4
3b2f:3b2e1a

The results of measurements of various statistical properties of the fluctuating wall-pressure field associated with turbulent subsonic boundary layer flow in conditions covering a range of values of boundary layer thickness and flow speed are given. The measured quantities include overall rms pressures, frequency spectra, and longitudinal and

P.T.O.

AGARD Report 455
North Atlantic Treaty Organization, Advisory Group for Aeronautical Research and Development
PROPERTIES OF THE FLUCTUATING WALL-PRESSURE FIELD OF A TURBULENT BOUNDARY LAYER
M.K. Bull
1963
34 pp., incl. 5 refs., 20 figs & discussion

532.526.4
3b2f:3b2e1a

The results of measurements of various statistical properties of the fluctuating wall-pressure field associated with turbulent subsonic boundary layer flow in conditions covering a range of values of boundary layer thickness and flow speed are given. The measured quantities include overall rms pressures, frequency spectra, and longitudinal and

P.T.O.

lateral space-time correlations in both broad and narrow frequency bands. Some experimental values of space-time correlation between wall-pressure fluctuations and turbulent velocity fluctuations at various positions in the boundary layer are also presented.

These experimental results and some of their implications on the structure of the wall-pressure field and the nature of its convection and decay are discussed.

This Report is one in the Series 448-469 inclusive, presenting papers, with discussions, given at the AGARD Specialists' Meeting on 'The Mechanism of Noise Generation in Turbulent Flow' at the Training Center for Experimental Aerodynamics, Rhode-Saint-Genèse, Belgium, 1-5 April 1963, sponsored by the AGARD Fluid Dynamics Panel.

lateral space-time correlations in both broad and narrow frequency bands. Some experimental values of space-time correlation between wall-pressure fluctuations and turbulent velocity fluctuations at various positions in the boundary layer are also presented.

These experimental results and some of their implications on the structure of the wall-pressure field and the nature of i convection and decay are discussed.

This Report is one in the Series 448-469 inclusive, presenting papers, with discussions, given at the AGARD Specialists' Meeting on 'The Mechanism of Noise Generation in Turbulent Flow' at the Training Center for Experimental Aerodynamics, Rhode-Saint-Genèse, Belgium, 1-5 April 1963, sponsored by the AGARD Fluid Dynamics Panel.

lateral space-time correlations in both broad and narrow frequency bands. Some experimental values of space-time correlation between wall-pressure fluctuations and turbulent velocity fluctuations at various positions in the boundary layer are also presented.

These experimental results and some of their implications on the structure of the wall-pressure field and the nature of its convection and decay are discussed.

This Report is one in the Series 448-469 inclusive, presenting papers, with discussions, given at the AGARD Specialists' Meeting on 'The Mechanism of Noise Generation in Turbulent Flow' at the Training Center for Experimental Aerodynamics, Rhode-Saint-Genèse, Belgium, 1-5 April 1963, sponsored by the AGARD Fluid Dynamics Panel.

lateral space-time correlations in both broad and narrow frequency bands. Some experimental values of space-time correlation between wall-pressure fluctuations and turbulent velocity fluctuations at various positions in the boundary layer are also presented.

These experimental results and some of their implications on the structure of the wall-pressure field and the nature of its convection and decay are discussed.

This Report is one in the Series 448-469 inclusive, presenting papers, with discussions, given at the AGARD Specialists' Meeting on 'The Mechanism of Noise Generation in Turbulent Flow' at the Training Center for Experimental Aerodynamics, Rhode-Saint-Genèse, Belgium, 1-5 April 1963, sponsored by the AGARD Fluid Dynamics Panel.